High-Pressure Photochemistry and Ultraviolet Spectroscopy in Gas–Liquid Systems

MARLIS F. MIRBACH,* MANFRED J. MIRBACH, and ALFONS SAUS

Universität Duisburg, GH-Fachbereich 6, Angewandte Chemie, Lotharstrasse 63, D-4100 Duisburg 1, West Germany

Contents

I. Introduction

This review summarizes the literature on high-pressure photochemical systems which consist of a gas and a liquid phase. The term "high pressure" means pressures above normal, and both photochemical reactions and photophysical processes are considered. There is no previous pertinent review covering this aspect, although there are a number of summaries on high-pressure photoreactions in the condensed phase.[1-6] Since there is no easy access to the literature on this topic in *Chemical Abstracts* or other secondary literature sources, the review is based on papers collected by the authors during their own work in this field. This literature is covered up to the middle of 1981. We would like to thank all colleagues who provided us with information and wish to apologize to those whose work did not come to our attention.

When a gas and a liquid are in equilibrium, a certain amount of the gas is dissolved in the liquid. In such a two-phase system, an increased pressure leads to an increased concentration of the gaseous compound in the liquid phase. Due to this additional amount of material the volume of the liquid phase is frequently also increased. Thus a decrease in density and internal pressure of the solution may result. These effects are opposite to those observed when a condensed-phase system is compressed, in which case the density increases and the volume decreases. A further difference is the much higher compressibility of a gas compared to a liquid which necessitates stringent safety precautions.

Since all of the photochemical and photophysical processes described in this article occur in the solution phase between the dissolved gas and another component, the only pressure effect which must be considered is the solubility of the gas in the solution. The applied pressures in gas–liquid systems range from 1 bar to a few hundred bars. Higher pressures are not usually necessary, since they would not increase the concentration of the gas in the solution. Investigations into the effects of high pressure in condensed systems normally require much higher pressures (between 1 and 10 kbar for liquids and 10 kbar to 1 Mbar for solids). The differing pressures required in condensed systems and in gas–liquid systems also reflect the fundamental differences of the pressure effects in each system. High pressure in the condensed system changes the rate constant of a chemical reaction. This may be described by eq 1,[7,8] where k = rate constant, P = pressure, $\Delta V^{\ddagger}$

$$(\partial \ln k/\partial P)_T = -V^{\ddagger}/RT \tag{1}$$

= activation volume, R = gas constant, and T = temperature.

In a gas–liquid system pressure does not alter the rate constant but changes the concentration of the gaseous compound in the solution. The consequence is a change in the reaction rate (eq 2) and/or in the chemical equilibrium (eq 3), where [G] = concentration of dis-

$$\text{reaction rate} = k[G]^u[L]^w \tag{2}$$

$$K = \frac{[\text{products}]^x}{[G]^u[L]^w} \tag{3}$$

solved gas, [L] = concentration of another compound in solution, u and w = partial reaction orders, and K = equilibrium constant.

In the literature there is also a very large number of reports dealing with the influence of pressure on pho-
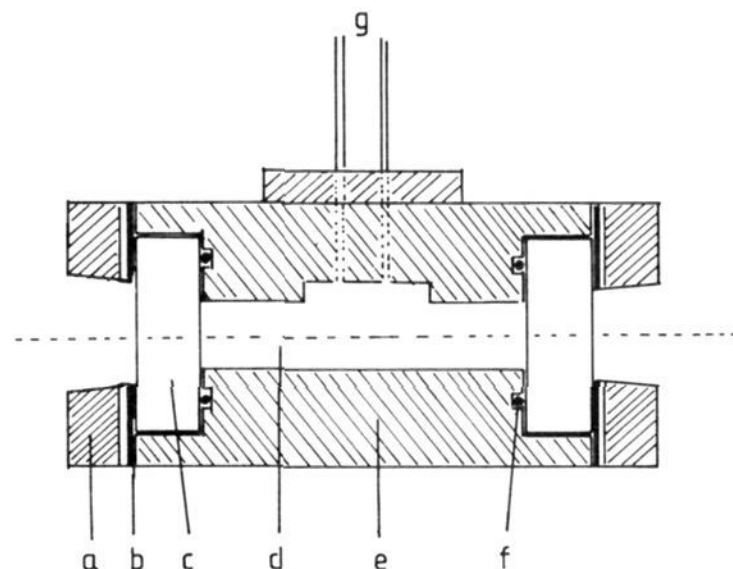
Figure 1. High-pressure UV cell (schematic). a = cover, b = teflon gasket, c = quartz window, d = sample compartment, e = cell housing, f = O-ring, g = gas in- and outlet.

tochemical and photophysical processes in the gas phase. In these examples the pressure applied usually ranges from a high vacuum to several hundred torrs, but also pressures up to 1000 bar have been studied.[9] In these systems high pressure increases the number of molecular collisions and is mainly used to study intramolecular reactions or deactivation processes. These gas-phase systems are also not considered in this review.

As already mentioned, the solubility of the gas in the liquid is the decisive factor of the reactions described in this review. Therefore in each chapter examples of solubilities are given. More details can be found in the reference works cited.

II. Experimental Techniques

Photochemical experiments require apparatus which is transparent to the radiation used. This may be achieved by using either pressure vessels made entirely from transparent material (e.g., glass) or metal pressure vessels fitted with relatively small windows.

Photochemical experiments in gas–liquid systems require an efficient mixing between the liquid and the gas phase. Because of the high compressibility of gases it is more or less necessary to maintain certain safety procedures which would be unnecessary in experiments with condensed-phase systems.

Transparent pressure vessels are usually made from glass or quartz tubes, the diameter and wall thickness of which depend upon the desired pressure. They have the advantage that they are easy to make and handle. They may only be used, however, for small volumes and relatively low pressures (up to 100 bar). This type of high-pressure photochemical apparatus has been used by Strohmeier[10,11] in the catalytic hydrogenation of cyclohexadiene, by Krusic[12,13] for investigations of metal carbonyls under hydrogen pressure, and by Wilson[14] for reactions of biradicals with oxygen.

More common and applicable to higher pressures are vessels made from stainless steel or brass and fitted with one or more windows. Various constructions are in use. They are usually homemade and adapted to the special requirements of the researchers. [Some UV cells and autoclaves are also commercially available. A list of suppliers may be obtained from the authors.]

UV spectra are usually measured in high-pressure cells similar to the one used by Evans[15] (see Figure 1). The cell consists of a flanged brass tube fitted with two

Marlis F. Mirbach was born in Mönchengladbach, West Germany, in 1947. She studied chemistry at the Technische Hochschule Aachen, where she received a doctorate with Alfons Saus in 1976. Following postdoctoral work with Nicholas J. Turro at Columbia University, she started as an author at the Gmelin-Institut of the Max-Planck-Society. In 1978 she joined the University of Duisburg, where she now works as an Assistant in the Department of Applied Chemistry. Her research interests include organometallic reaction mechanisms, photo- and radiation chemistry of organic and organometallic compounds, and homogeneously catalyzed reactions induced by light.

Manfred J. Mirbach was born in Würselen, West Germany, in 1945. He studied at the Technische Hochschule Aachen, where he received a doctoral degree in chemistry in 1976 under Alfons Saus. He did postdoctoral work on organic photochemistry at Columbia University with Nicholas J. Turro and at the Max-Planck-Institut für Strahlenchemie in Mühlheim/Ruhr. Between 1978 and 1980 he worked in a research project on radiation chemistry under Alfons Saus at the Technische Hochschule Aachen, and in 1981 he joined the Department of Applied Chemistry at the University of Duisburg, where he works now as an Assistant. His research interests include photochemistry and radiation chemistry of organic and organometallic compounds and especially catalytic reactions under pressure induced by light.

Alfons Saus was born in Lohn, West Germany, in 1931. He studied in Aachen, Karlsruhe, and Berlin and did his thesis work on heterocyclic compounds at the Technische Hochschule Aachen under the direction of Friedrich Asinger. Then he specialized in radiochemistry and radiation chemistry and ran the division of radiation chemistry at the Technische Hochschule Aachen from 1965 to 1980. He did research on the radiation-induced telomerization of olefins, cycloaddition reactions, hydroformylation, and homologation. In 1977 he took over the newly founded Department of Applied Chemistry at the University of Duisburg, where he is now active in the fields of homogeneous and heterogeneous catalysis.

0.25-in.-thick plate-glass windows, each bolted between 0.25-in.-thick PTFE gaskets.[15,16] Nowadays similar cells are normally made from stainless steel and use quartz or fused silica windows for better transmission in the
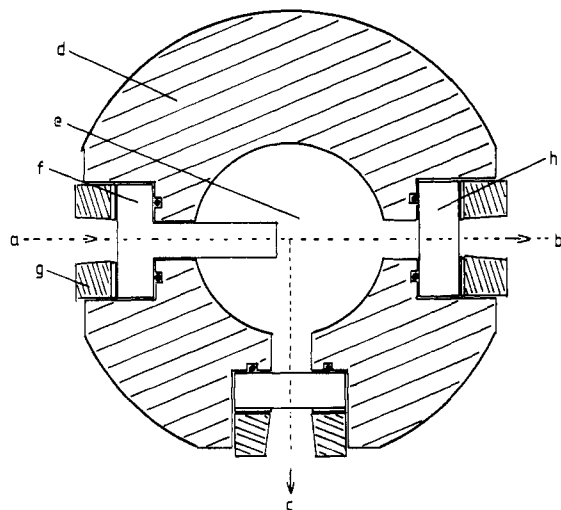
Figure 2. Scheme of a fluorescence cell (after Lakowicz and Weber[25]). a = excitation beam, b = transmission beam, c = emission beam, d = steel cell housing, e = sample compartment, f = T-shaped quartz window, g = holding screw, h = cylinder-shaped quartz window.

UV range. (For further descriptions, see ref 17–22.) The different methods of window mounting are discussed elsewhere.[23] For gas–liquid systems with pressures of a few hundred bars, the window is normally sealed by PTFE or Viton O-rings. The cell is filled with enough liquid to cover the windows and gas is introduced to the desired pressure to record a spectrum.

The cells discussed up to now have only a small volume of vapor phase above the liquid. Therefore several cycles of shaking and pressurizing are necessary, and the time required for a complete equilibration between the gas and liquid phase to be reached is rather long. Therefore it may be advantageous to equilibrate the solution in a separate vessel and transfer the solution afterward to the optical cell via a high-pressure steel capillary.[24]

To measure fluorescence spectra Lakowicz and Weber[25] developed a cell with windows arranged orthogonally. Special T-shaped windows have been used (Figure 2) to guarantee a maximum light absorption in the center of the cell.

A different design for front-face measurements of fluorescence spectra has been used by Grabowski et al.[26] (Figure 3). This mode of measurement has advantages for samples with high optical density, high scatter, or low quantum yields. The focusing and collimating system was described by Jasny.[27]

So that contact between the liquid and the cell wall can be avoided or when small quantities of liquid are to be measured, a conventional optical glass cell may be placed into the pressure vessel[25,28] (Figure 4). Under this method with 1-cm optical cells the time required to equilibrate gas and liquid phases is particularly long. Wiht a 2-cm-square cuvette 30–60 min is needed for equilibration.[25]

For chemical reactions the high-pressure cells described so far have two significant disadvantages: (a) there is no forced mixing between the gas and the liquid phase; (b) due to the use of small windows, only a small fraction of the radiation from the external light source actually reaches the sample. Therefore reactions can be performed on a limited scale only and usually require long reaction times.
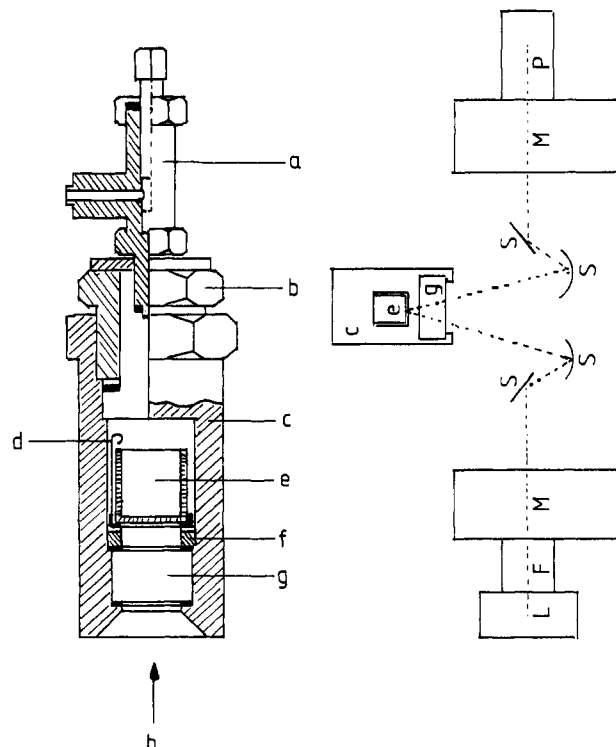

Figure 3. Scheme of a fluorescence cell (after Grabowski et al.[26]). a = needle valve, b = cell lid, c = cell housing, d = cell holder, e = quartz cell, f = holding ring, g = quartz window, h = excitation beam, L = lamp, F = focusing system, M = monochromator, S = mirror, P = phototube.
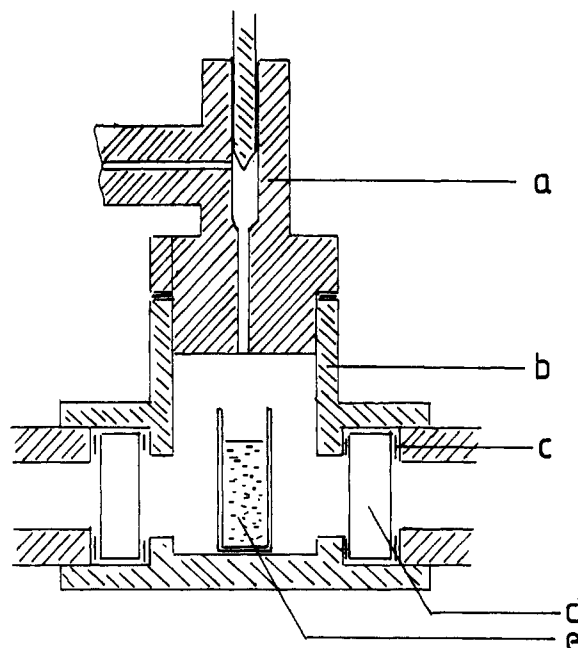

Figure 4. High-pressure UV cell (after Grabowski[28]). a = needle valve, b = cell housing, c = Teflon ring, d = quartz window, e = optical quartz cell.

Photoreactions on a preparative scale are better performed in a UV autoclave[29-31] which overcomes the limitations mentioned under (a) and (b). Figure 5 shows the principle of this construction. The lamp is located in the center of the reaction medium and is protected against the high pressure by a quartz or pyrex tube. Glass or quartz tubes can stand much higher pressures on the outside than on the inside, since they
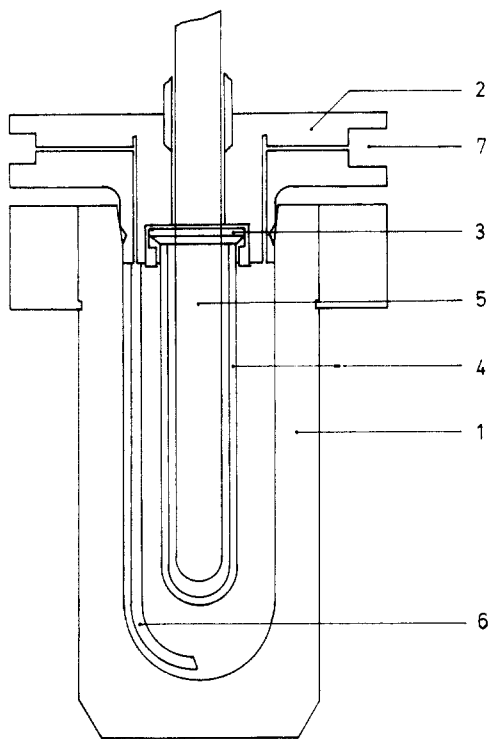
Figure 5. UV autoclave (after Saus[31]). a = autoclave lid, b = gas in- and outlet, c = packing, d = lamp, e = pressure stable quartz tube, f = autoclave housing, g = sampling tube.
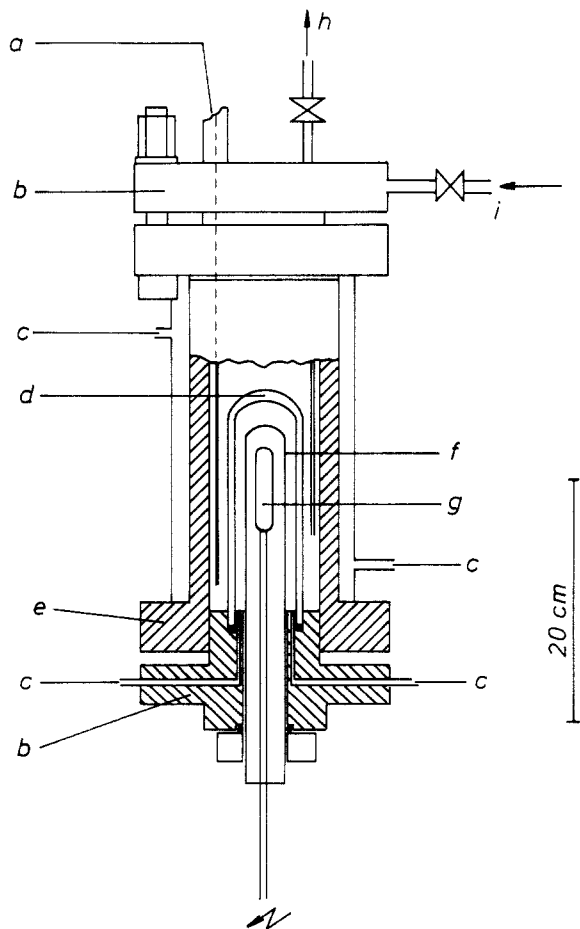

Figure 6. UV autoclave (after Gascard and Saus[33]). a = magnetic stirrer, b = autoclave lid, c = connection to thermostat, d = pressure-stable quartz tube, e = autoclave housing, f = quartz or Pyrex tube, g = lamp, h = gas entrance and sampling valve, i = gas outlet.
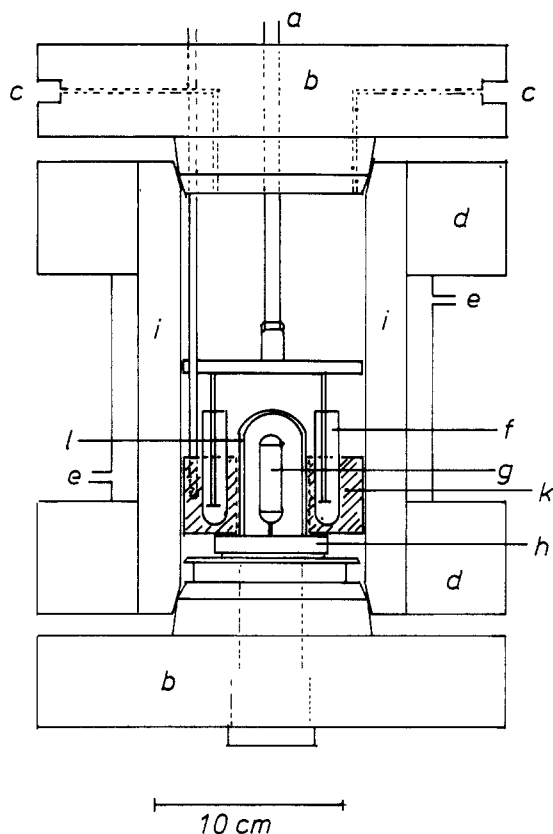

Figure 7. Multiple sample UV autoclave.[69b] a = magnetic stirrer, b = autoclave lid, c = gas exit and entrance, d = flange, e = connection to thermostat, f = sample test tube, g = lamp, h = quartz tube holder, i = autoclave housing, k = sample holder, l = pressure-stable quartz tube.

withstand considerably higher compressive than tensile stresses.[23] Mixing is achieved either by rocking the whole autoclave[30] or by circulating the gas through the solution with an external high-pressure centrifugal pump.[32]

A more advanced design uses a magnetically driven up and down stirrer. The lamp is introduced from the bottom of the vessel and is separated from the solution by a double-walled quartz or Pyrex tube which allows the lamp to cool[33-35] (Figure 6). Both high-pressure (up to 700 W) and low-pressure mercury lamps may be used with this type of UV autoclave.

To carry out a chemical reaction one fills the autoclave with 300 to 600 mL of solution. This leaves enough gas phase above the solution to maintain a practically constant pressure, even though some of the gas is used up during the reaction. Furthermore, a modified type of this UV autoclave permits the irradiation of up to six samples at a time (Figure 7).[35] Its use, however, is restricted to solutions of low volatility.

Quantum yields of photochemical reactions under pressure can be determined with a UV microreactor which contains 1 mL of liquid phase and 4 mL of gas phase. Mixing is achieved with a stirring bar and a magnetic stirrer (Figure 8). Monochromatic light may be produced by using either a monochromator or lasers.[36]

It should be noted that, for quantitative measurements, a correction is necessary for the dilution effect. This dilution occurs upon increase of the volume of the liquid phase due to the gas dissolving under high pressure.
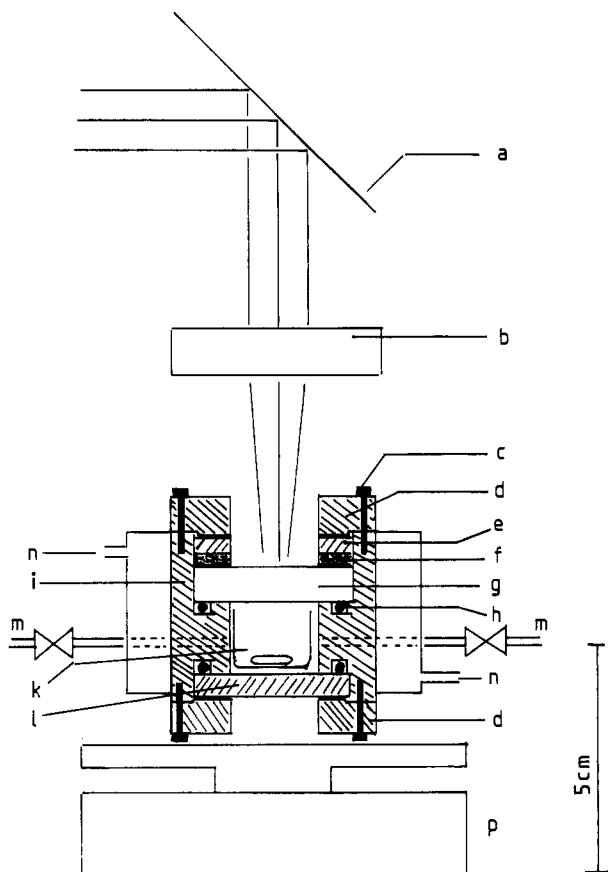
Figure 8. High-pressure quantum yield cell.[36] a = mirror, b = focusing lens, c = screws, d = cover, e = aluminum ring, f = Teflon ring, g = quartz window, h = O-ring, i = cell housing, k = glass insert, sample compartment, l = stainless steel disc, m = gas in- and outlet, n = connection to thermostat, p = magnetic stirrer.

Figure 9. Oxygen-perturbed UV absorption spectrum of trans-dicyanoethylene (pathlength 5.2 cm).[24] (a) 2 M trans-di-cyanoethylene in CH_2Cl_2 + 150-bar O_2, (b) 2 M trans-dicyano-ethylene in CH_2Cl_2 without oxygen, (c) spectrum a - spectrum b.

TABLE I. Solubility of Oxygen in Various Solvents

		solubility		
solvent	pressure, bar	[mol/L]	[cm³ of gas/ cm³ of solvent]	ref
n-pentane	100	2.5	58	37a
Freon 113	100	4.2	95	18
water	100	0.13	3	25
water-d_2	1, air-sat.	0.0003		58
water-d_2	100	0.12		58
CCl_2F-$CClF_2$	144	3.6	81	57

III. High Pressure of Oxygen

A. Oxygen Solubility

The solubility of oxygen in inert solvents increases with increasing pressure, closely following Henry's law. Examples of oxygen concentrations in several solvents at increased pressures are listed in Table I.

B. Singlet–Triplet Perturbation Spectra

High pressures of oxygen have long been known to enhance the $S_0 \rightarrow T_1$ absorption of some organic molecules. This oxygen perturbation effect is particularly strong for aromatic and olefinic hydrocarbons, for which the singlet–triplet absorption is strongly forbidden. Compounds containing heavy atoms or possessing an n,π* lowest excited state do not usually show enhanced singlet–triplet absorption in the presence of oxygen. The $S_0 \rightarrow T_1$ π,π* absorption is generally enhanced by
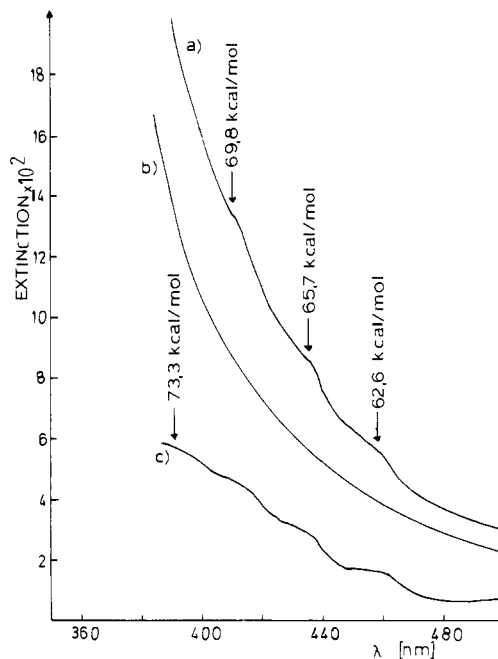
spin–orbital perturbation. Compounds possessing lowest n,π* states or heavy atoms are not generally sensitive to spin–orbit perturbations, because they already possess a substantial spin–orbit interaction.

The efficiency of the oxygen effect depends on the oxygen concentration and may be expressed as $k_{ST}^{O_2}[O_2]$, where $k_{St}^{O_2}$ is a bimolecular rate constant for oxygen perturbation and $[O_2]$ is the concentration of oxygen in the sample. The solubility of oxygen in many organic solvents is about 10^{-2} mol/L at 1 bar of oxygen, and typical values for $k_{ST}^{O_2}$ are $\sim 10^{10}$–10^9 M^{-1} s^{-1}. Thus $k_{ST}^{O_2}[O_2] = 10^8$–10^7 s^{-1}. The oxygen solubility at 140 bar may be as high as 3.5 mol/L, resulting in $k_{ST}^{O_2}[O_2] = 10^{10}$–$10^9$ s^{-1}. Thus it is possible to enhance the oscillator strength of a spin-forbidden transition by a factor of 100 by dissolving oxygen under high pressure.[38a]

The practical application of the high-pressure oxygen technique was introduced by Evans[15,21,39–42] and has been employed to locate or confirm the triplet levels of a large number of aromatic hydrocarbons and polyenes. $S_0 \rightarrow T_1$ absorption spectra are especially helpful to gain information about compounds which do not phosphoresce. A number of data on triplet energies obtained by this method is listed in Table II.

For a typical example of a $S_0 \rightarrow T_1$ transition which is enhanced by oxygen the reader is referred to the absorption spectrum of trans-dicyanoethylene in Figure 9.[24] Figure 10 shows the $S_0 \rightarrow T_1$ absorption spectrum of an azo compound having a lowest n,π* triplet state. This absorption is not changed by high pressure of oxygen.[51]

Grabowska et al.[52] calculated the change of the acid–base equilibrium of N-containing heterocyclic compounds upon excitation to the triplet state. The experimental method is based on Förster's cycle (eq 4),

$$pK^* = pK_g - (E_{BH^+} - E_B)/(Rt \ln 10) \quad (4)$$

TABLE II. Energies of $S_0 \rightarrow T_1$ Transitions Determined by the Oxygen Perturbation Method[a]

compound	solvent; pressure, bar	ν, cm^{-1}	ref
olefins			
ethylene	vapor; 25	28 700	40
	CH_2Cl_2; 150	27 550	24
trans-d_2	vapor; 25	28 800	40
d_4	vapor; 30	28 940	40
trans-1,2-dichloro	neat; 30, 120	27 800	28
cis-1,2-dichloro	neat; 30, 120	$\geqslant$ 28 500	28
trans-dicyano	CH_2Cl_2; 150	~ 22 000	24
maleic anhydride	CH_2Cl_2; 150	$\geqslant$ 25 600	24
dimethyl maleate	CH_2Cl_2; 150	f	24
dimethyl fumarate	CH_2Cl_2; 150	~ 23 600	24
dienes			
1,3-butadiene	$CHCl_3$; 150	20 920	44
	$CHCl_3$; 130	20 830	40
	vapor; 130	22 100[c]	40
1-chloro	$CHCl_3$; 150	19 880	44
2-chloro	$CHCl_3$; 150	20 490	44
2,3-dichloro	$CHCl_3$; 150	20 580	44
1-methoxy	$CHCl_3$; 150	19 800	44
cis-1,3-pentadiene	$CHCl_3$; high	20 070	43
trans-1,3-pentadiene	$CHCl_3$; 150	20 700	44
isoprene	$CHCl_3$; 130	21 000	40
	$CHCl_3$; 150	21 000	44
cyclopentadiene	$CHCl_3$; 150	20 330	44
	$CHCl_3$; 130	20 400	40
2,4-hexadiene	$CHCl_3$; 150	20 530	44
1-hydroxy	$CHCl_3$; 150	20 790	44
2,3-dimethylbutadiene	$CHCl_3$; 150	21 150	44
1,3-cyclohexadiene	$CHCl_3$; 130	18 700	40
	$CHCl_3$; 150	18 350	44
	CH_2Cl_2; 170	18 100	48
polyenes			
trans-1,3,5-hexatriene	$CHCl_3$; 130	16 450	40
octa-2,4,6-trienal	$CHCl_3$; 130	15 210	40
deca-2,4,6,8-tetraenal	$CHCl_3$; 130	12 700	40
dodeca-2,4,6,8,10-pentaenal	$CHCl_3$; 130	11 050	40
2,2'-bis(dibutadiene)	$CHCl_3$; 150	20 280	44
acetylenes			
acetylene	vapor; 100	explosion	40
1,3-butadiyne	vapor; 130	27 020	40
	$CHCl_3$; 130	27 300	40
2,4-hexadiyne	$CHCl_3$; 130	27 910	40
1,3-hexadiyne	$CHCl_3$; 130	27 420	40
5,7-dodecadiyne	$CHCl_3$; 130	27 820	40
1,6-dichloro-2,4-hexadiyne	$CHCl_3$; 130	26 460	40
1,6-dihydroxy	$CHCl_3$; 130	27 380	40
2,4,6-octatriyne	$CHCl_3$; 130	22 170	40
aromatics			
benzene	neat; 0.89	29 440	15
	vapor; 130	29 510	21
	vapor; 130	29 542	97
	vapor; 170	29 500	17
fluoro	neat; 0.91	29 500	15
	vapor; 140	29 530	21
	vapor; 170	29 400	17
o-difluoro	vapor; 170	29 300	17
p-difluoro	vapor; 170	29 000	17
m-difluoro	vapor; 170	29 500	17
1,3,5-trifluoro	vapor; 170	29 900	17
1,2,4-trifluoro	vapor; 170	29 300	17
1,2,3,4-tetrafluoro	vapor; 170	29 200	17
1,2,3,5-tetrafluoro	vapor; 170	29 600	17
1,2,4,5-tetrafluoro	vapor; 170	29 000	17
pentafluoro	vapor; 170	29 200	17
hexafluoro	vapor; 170	29 100	17
chloro	vapor; 130	28 570	39
benzonitrile	$CHCl_3$; 130	26 880	39
toluene	vapor; 170	28 800	17
	TMP;[g] 130	29 000	39
p-fluoro	vapor; 170	28 500	17
benzotrifluoride	TMP; 130	29 150	39
	vapor; 130	29 150	39
o-xylene	vapor; 170	28 300	17
m-xylene	vapor; 170	28 400	17

TABLE II (*Continued*)

compound	solvent; pressure, bar	ν, cm^{-1}	ref
p-xylene	vapor; 170	28 100	17
acetophenone	CHCl$_3$; 130	25 950	39
4-hydroxy	CHCl$_3$; 100	24 690	16
4-methoxy	CHCl$_3$; 100	25 190	16
benzoyl chloride	CHCl$_3$; 130	26 280	39
biphenyl	CHCl$_3$; 45	f	15
MeSO$_2$C$_6$H$_5$	CHCl$_3$; 130	28 700	39
phenylcyclopropene	CHCl$_3$; 130	28 300	39
α-tocopherol	Freon; 100	29 500	18
		(23 500)^d	
styrene	CHCl$_3$; 76	21 600	15
	F-MCH;^{h} 180	21 600	49
trans-β-methyl	CHCl$_3$; high	21 050	43
	F-MCH; 180	20 830	49
cis-β-methyl	F-MCH; 180	22 990	49
trans-β-*tert*-butyl	F-MCH; 180	21 740	49
cis-β-*tert*-butyl	F-MCH; 180	22 990	49
α-methyl	F-MCH; 180	21 740	49
1-phenylcyclopentene	F-MCH; 180	20 830	49
3-phenylpropene	F-MCH; 180	28 170	49
diphenylbutadiene?	CHCl$_3$; 76	14 700?	15
phenylacetylene	CHCl$_3$; 130	25 190	39
trans-stilbene	CHCl$_3$; 76	17 750	15
	CHCl$_3$; 140	17 400	50
	benzene; 120	17 700	59
cis-stilbene	CHCl$_3$; 76	c	15
	benzene; 120	$\sim$19 000^c	59
trans-α-methylstilbene	CHCl$_3$; high	$\sim$17 600	43
4 methoxy *trans*-stilbene	CHCl$_3$; 140	17 550	50
4-methoxy-4'-NMe$_2$	CHCl$_3$; 140	f	50
4-Ph$_2$P=O	CHCl$_3$; 140	17 500	50
4-Ph$_2$P=O,4'-OMe	CHCl$_3$; 140	17 150	50
4-Ph$_2$P=O,3'-OMe	CHCl$_3$; 140	17 500	50
4-Ph$_2$P=O,2'-OMe	CHCl$_3$; 140	17 400	50
4-Ph$_2$P=O,4'-NMe$_2$	CHCl$_3$; 140	f	50
4-Ph$_2$P=O,3'-NMe$_2$	CHCl$_3$; 140	f	50
1,6-diphenylhexatriene	CDCl$_3$; 137	12 450	54
1,8-diphenyloctatetraene	CDCl$_3$; 137	11 050	54
diphenylacetylene	CHCl$_3$; 75	21 860	15
naphthalene	CHCl$_3$; 76	21 180	15
1-bromo	CHCl$_3$; 75	20 650^b	15
1-acetyl	CHCl$_3$; 100	19 760	16
2-acetyl	CHCl$_3$; 100	20 580	16
1-formyl	CHCl$_3$; 100	19 600	16
2-benzoyl	CHCl$_3$; 100	20 830	16
anthracene	CHCl$_3$; 93	14 870	15
9-methyl	CHCl$_3$; 76	14 460	15
9-nitro	CHCl$_3$; 75	14 630	15
9-formyl	CHCl$_3$; 100	15 200	16
1-chloro	CCl$_2$F–CClF$_2$; 137	14 700	54
fluorene	CHCl$_3$; 76	23 580	15
phenanthrene	CHCl$_3$; 47	21 600	15
fluoranthrene	CHCl$_3$; 76	18 450	15
1,2:3,4-dibenzanthracene	CHCl$_3$; 76	17 790	15
pyrene	CHCl$_3$; 50	16 930	15
3,4-benzopyrene	CHCl$_3$; 76	14 670	15
anthanthrene	CHCl$_3$; 137	11 800	54
tetracene	CHCl$_3$; 137	10 420?	54
5-methyl	CDCl$_3$; 137	10 170	54
heterocycles			
acridine	CHCl$_3$; 75	15 840	15
pyridine	CHCl$_3$; 135	29 650	21
	TMP; 90	29 650	21
	ethanol; 135	$\sim$30 000	21
quinoline	CHCl$_3$; 130	21 850	39
	ethanol; 130	$\sim$22 000	52
isoquinoline	CHCl$_3$; 130	21 210	39
7,8-benzoquinoline	CHCl$_3$; 130	21 740	39
5,6-benzoquinoline	CHCl$_3$; 130	21 880	39
pyrazine	TMP; 130	26 600^b	39
phenazine	benzene; 135	$\sim$17 000^b	45
		15 600	
	ethanol; 130	$\sim$15 500^b	52
phenazine-H$^+$	ethanol; 130	$\sim$14 000^b	52
quinoline-H$^+$	ethanol; 130	$\sim$21 500	52
thionaphthene	CHCl$_3$; 130	23 970	39
9-anthroylacetone	CHCl$_3$; 130	14 620	41

TABLE II (*Continued*)

compound	solvent; pressure, bar	ν, cm^{-1}	ref
tris(9-anthroylacetonato)gadolinium	CHCl$_3$; 130	14 650	41
trans-azomethane	vapor; 155	19 500	47
trans-azoethane	vapor; 155	19 400	47
trans-azo-*n*-propane	CHCl$_3$; 155	19 500	47
trans-azoisopropane	CHCl$_3$; 155	19 900	47
1, eq 9	CHCl$_3$; *b, e*	21 000	51

a For completeness, spectra in the vapor phase are also included. The energies given refer to O–O transitions whenever possible. For unstructured absorption the absorption onset or the energy at one-third of the maximum intensity of the first band have been used as an approximation. *b* Detectable also in the absence of oxygen. *c* O–O band was unobservable. *d* Shoulder. *e* Not enhanced by 100-bar oxygen pressure. *f* No S$_0$ → T$_1$ absorption detectable. *g* TMP = 2,2,4-trimethylpentane. *h* F-MCH = perfluoromethylcyclohexane.
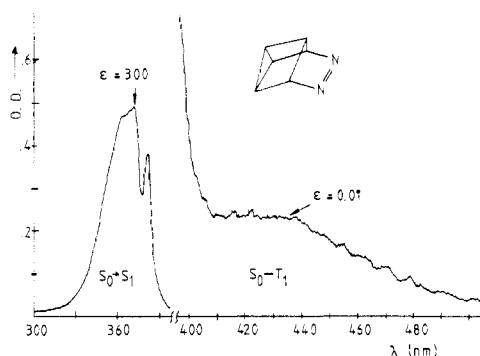
Figure 10. UV absorption spectrum of azo compound 1 in pentane.[51] S$_0$ → S$_1$ spectrum with 1-cm pathlength; S$_0$ → T$_1$ spectrum with 10-cm pathlength. The spectra are similar in the presence or absence of oxygen.

where pK_g refers to the ground-state equilibrium and E_B and E_{BH^+} are 0–0 transition energies of the free base and conjugate acid, respectively. The 0–0 transitions were determined from the phosphorescence and the oxygen-perturbed absorption spectra for quinoline (pK^* = 5.6, ΔpK = +0.6) and acridine (pK^* = 5.4, ΔpK = −0.1).

Dijkgraaf et al. observed a shoulder at 29 000 cm^{-1} in the absorption spectrum of a naphthalene solution saturated with oxygen under pressure.[53] They attributed this to a simultaneous transition in which the naphthalene is excited to its lowest triplet state and the oxygen undergoes a $^1\Delta_g \leftarrow {}^3\Sigma_g^-$ transition. In agreement with this interpretation, the separation between this shoulder and the 0–0 singlet–triplet band of naphthalene is 7900 cm^{-1}, as compared with the $^1\Delta_g \leftarrow {}^3\Sigma_g^-$ interval of 7882 cm^{-1} for oxygen in the gas phase. The assignment of the absorption is supported by further examples, e.g., solutions of anthracene,[42] 1-chloroanthracene, 5-methyltetracene, tetracene, 1,6-diphenylhexatriene, and 1,8-diphenyloctatetraene. The separations of the simultaneous transitions from the 0,0 bands of the S$_0$ → T$_1$ absorption for all solutions are found to be around 7800 cm^{-1}.[54] It is pointed out[42] that the short-wavelength bands observed in the oxygen perturbation spectra of butadiene, 1,3,5-hexatriene, and 1,3,5,7-octatetraene, which had been assigned as transitions to the second triplet levels of the organic molecules, are in fact also simultaneous transitions (see Figure 11 for an energy correlation diagram[55]). The strongly forbidden $^3\Sigma_g^- \rightarrow {}^3\Sigma_u^+$ transition of molecular oxygen is enhanced in the presence of 2 bar of ethylene or acetylene, but not in the presence of ethane. It should be noted that ethylene and acetylene are con-
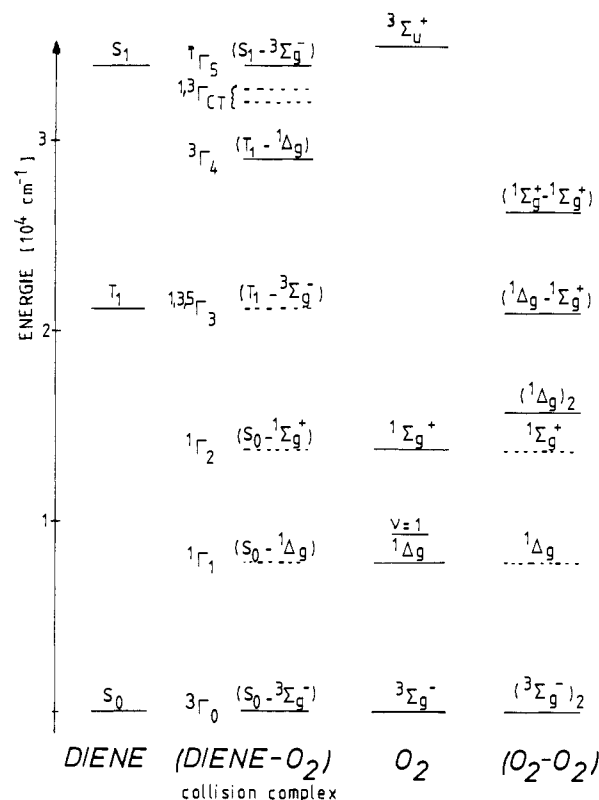

Figure 11. Schematic presentation of possible electronic transitions in dienes, oxygen, and diene–oxygen collision complexes.

siderably more effective in perturbing this transition than oxygen itself.[40]

C. Photochemical Generation of Singlet Oxygen

Many photooxidations involve low-lying singlet states of oxygen ($^1\Delta_g$ and $^1\Sigma_g^+$) as intermediates. Singlet oxygen can be produced by dye sensitization (e.g., with rose bengal) or by direct optical excitation, preferably at high pressures of oxygen dissolved in an inert organic solvent. The latter method is well suited to quantitative investigations and also has the advantage of high selectivity, since only the desired species is produced. In dye-sensitized photooxidations it is not always clear whether singlet oxygen is, in fact, involved (type II photooxygenation) or whether the excited state of the dye reacts with the substrate to give free-radical intermediates (type I photooxygenation).

The normal emission wavelength of a He–Ne laser (632.8 nm) almost exactly coincides with that of the oxygen $(^1\Delta_g)_2$–$(^3\Sigma_g^-)_2$ transition. Irradiation of a dilute solution of 9,10-dimethylanthracene in Cl$_2$FC–CF$_2$Cl

TABLE III. Production of Singlet Oxygen by Direct
Excitation of Molecular Oxygen[a]

method of production	reactant	result	ref
$(^3\Sigma_g^-)_2 \rightarrow (^1\Delta_g)_2$	DMA	$\phi = 0.13^b$	56
He–Ne laser, 130 bar	DMA	$\phi = 0.05^c$	
in $CCl_2F–CClF_2$	DPBF	$\phi = 0.06^d$	
$^3\Sigma_g^- \rightarrow {}^1\Delta_g$ or	DMA, DPBF	$\phi_{dimer} = 2 \times \phi_{monomer}$	
$(^3\Sigma_g^-)_2 \rightarrow (^1\Delta_g)$	DMA	$k_q/k_r = 0.6$	57
Nd–YAG or He–Ne laser	TPCPD	$k_q/k_r = 1.7$	
140 bar, in $CCl_2F–CClF_2$	DPDF	$k_q/k_r = 0–1$	
	NEt$_3$	$k_q/k_r = 11$	
$^3\Sigma_g^- \rightarrow {}^1\Delta_g$	DPBF	$k_r = 1.1 \times 10^9 \ M^{-1} s^{-1}$	58
Nd–YAG laser in water–SDS micelle		$\tau(D_2O) = 42 \ s$	
		$\tau(H_2O) = 3 \ s$	
		$K = 2.8$	
		$k_{in}{}^T = 1 \times 10^8 \ s^{-1}$	
		$k_{out}{}^T = 3.7 \times 10^7 \ s^{-1}$	
		$k_{in}{}^E = 9 \times 10^9 \ M^{-1} s^{-1}$	
		$k_{out}{}^E = 3 \times 10^9 \ M^{-1} s^{-1}$	
$^3\Sigma_g^- \ {}^1\Delta_g$	α-toco-pherol	$k_q = 3.1 \times 10^7 \ M^{-1} s^{-1}$	18
Nd–YAG laser in Freon 113		$k_r = 1.9 \times 10^6 \ M^{-1} s^{-1}$	
		$k_r/k_q = 0.061$	

[a] DMA = 9,10-dimethylanthracene; DPBF = 1,3-diphenylisobenzofuran; TPCPD = tetraphenylcyclopentadienone; NEt$_3$ = triethylamine. ϕ = quantum yield for singlet oxygen formation; k_q = rate constant for quenching; k_r = rate constant for reaction of singlet oxygen with reactant; τ = lifetime of singlet oxygen; K = partition constant for singlet oxygen between aqueous and micellar phase; $k_{in}{}^T$, $k_{out}{}^T$ = rate constants for transfer of singlet oxygen between aqueous phase and micelle at low oxygenconcentrations (by diffusion) $k_{in}{}^E$, $k_{out}{}^E$ = rate constants for transfer of singlet oxygen between aqueous phase and micelle at high oxygen concentrations (mainly by collisional electronic energy transfer). [b] At 1.8×10^{-4} M DMA. [c] At 4.4×10^{-5} M DMA. [d] At 9×10^{-6} M DPBF.

under 140-bar oxygen pressure with a He–Ne laser yields 9,10-dimethylanthracene peroxide (eq 5).[56] The


$$ (5) $$
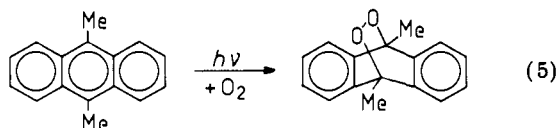
same reaction occurs when the $^1\Delta_g$ state of oxygen is selectively produced by the 1065-nm light of a Nd–YAG laser.[62] The reactivity of the $(^1\Delta_g)_2$ and $^1\Delta_g$ states of oxygen has been studied quantitatively in the reactions with 9,10-dimethylanthracene (eq 5) and 1,3-diphenylisobenzofuran (eq 6). The quantum yields for

$$ (6) $$
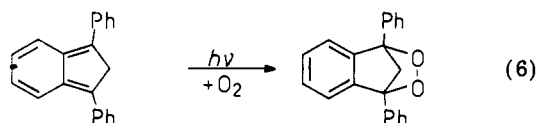
peroxide formation upon $(^1\Delta_g)_2$ excitation are twice those for $^1\Delta_g$ excitation. Beside the expected chemical reaction k_r, interaction of $O_2(^1\Delta_g)$ with substrates like dimethylanthracene (eq 5), tetraphenylcyclopentadienone (eq 7), 1,3-diphenylisobenzofuran (eq 6),

$$ (7) $$
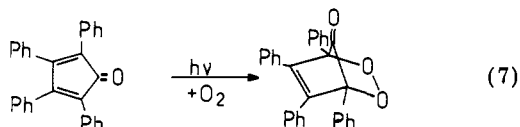
or α-tocopherol (eq 8) leads also to physical quenching

$$ \alpha\text{-tocopherol} + {}^1O_2 \rightarrow \text{endoperoxide intermediate} \tag{8} $$
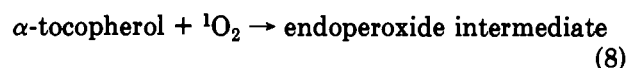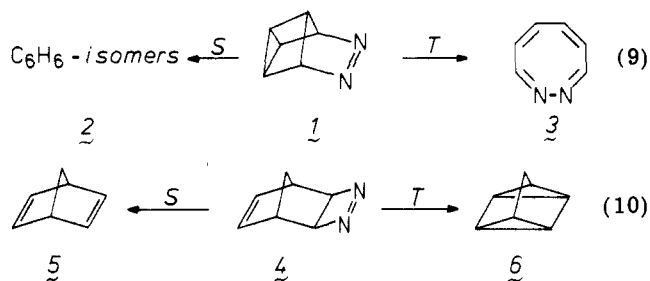
of the singlet oxygen (k_q).[18,57,58] These results are summarized in Table III.

D. Chemical Reactions from Oxygen-Assisted Produced Triplet States

The triplet state of organic molecules is an important intermediate in photochemical reactions. Usually the quenching of triplet sensitizers is used for selectively populating the triplet state of a reactant. There are few examples where the triplet state is populated by irradiation within the singlet–triplet absorption band in the presence of oxygen. In one case the photoisomerization of 1,2-dichloroethylenes was investigated[28] and in the other case the cis–trans isomerization of stilbene.[59] When the cis- or trans-dichloroethylenes are irradiated by the full spectrum of a high-pressure mercury arc, side reactions take place along with photoisomerization, viz., formation of a nonvolatile residue (possibly polymer?) accompanied by evolution of HCl. Excluding the wavelengths below 290 nm with a filter eliminates the side reactions. The photochemically active radiation is then only that absorbed within the oxygen-induced absorption band in the range 400–300 nm. Isomerization resulting from the selective excitation to the triplet state occurs with high quantum yields; e.g., for the trans–cis conversion the quantum yield is $\phi_{ct} = 0.61 \pm 0.07$, and for the reverse isomerization $\phi_{tc} = 0.45 \pm 0.06$. The experimental result $\phi_{ct} + \phi_{tc} = 1.06 \pm 0.13$ indicates that only one triplet state, common to both isomers, is active in the photoisomerization. The intermediate state is reckoned to correspond to an angle of twist about 90° and to a considerable stretching of the C–C bond.[28]

When cis-stilbene is selectively excited to its lowest triplet state, it does not undergo any cyclization reaction and, even in the presence of high concentrations of oxygen, no phenanthrene is formed. This supports the singlet mechanism of the photocyclization. A selective excitation of cis- or trans-stilbene to the lowest triplet state (excitation wavelengths around 405 nm) leads to an isomerization with quantum yields of $\phi_{ct} = 0.22 \pm 0.04$ and $\phi_{tc} = 0.42 \pm 0.03$, respectively. The values are in accord with those found in photosensitization experiments. Strikingly, the sum of the quantum yields of the forward and reverse reaction is less than unity, which indicates the existence of more than one minimum on the energy hypersurface of the stilbene triplet. The existence of two nonequivalent energy minima in twisted configurations is proposed for the lowest triplet state.[59]

The perturbation of singlet–triplet transitions is not limited to $S_0 \rightarrow T_1$ absorption but may also be used to enhance the rate of S_1 to T_1 intersystem crossing. This was demonstrated with azo compound 1, which produces the benzene isomers 2 upon direct excitation to the singlet state. Under 100 bar of oxygen direct excitation leads to 85% formation of 3 the typical triplet product (eq 9). Similar results were obtained with azo compound 4 (eq 10), which forms mainly norbornadiene

$$C_6H_6 - \textit{isomers} \xleftarrow{\ S\ } \underset{\underset{\sim}{2}}{\boxed{}} \xrightarrow{\ T\ } \underset{\underset{\sim}{3}}{\boxed{}} \quad (9)$$

$$\underset{\underset{\sim}{5}}{\boxed{}} \xleftarrow{\ S\ } \underset{\underset{\sim}{4}}{\boxed{}} \xrightarrow{\ T\ } \underset{\underset{\sim}{6}}{\boxed{}} \quad (10)$$

5 upon direct excitation in the absence of oxygen. Under oxygen pressure, however, the typical triplet product quadricyclene **6** is formed in 95% yield.[51]

E. Quenching of Excited States by Oxygen

Ground-state molecular oxygen ($^3\Sigma_g$) is a general and efficient quencher of the S_1 and T_1 states of organic molecules. In general, quenching of the S_1 state of aromatic hydrocarbons occurs at close to diffusion rates. An interesting feature of diffusional quenching by $^3O_2$ is that this diatomic species diffuses considerably faster than most organic molecules. For example, in benzene near room temperature, oxygen diffuses two to three times faster than anthracene. Another important practical feature of quenching by molecular oxygen is its low solubility in most organic solvents: with an oxygen concentration of $[O_2] \sim 10^{-2}$ M at 760 mm and a quenching rate constant of $k_q \sim 10^{10}$ M^{-1} s^{-1}, then $k_q[O_2] \leq 10^8$ s^{-1} at ordinary pressures. Thus S_1 or T_1 states with decay rates of the order of 10^8–10^9 s^{-1} will not be efficiently quenched in air-saturated solutions and will be only moderately quenched in oxygen-saturated solutions.[38b]

There are only few reports on oxygen quenching processes in aqueous solutions. This is probably due to the low solubility and diffusion coefficient of oxygen in water compared to organic solvents. This problem may be overcome with increased concentration of oxygen due to an increase in the oxygen pressure. Equilibration of an aqueous solution with oxygen at a pressure of 100 bar results in a concentration of dissolved oxygen (0.13 M)[25] which is sufficient to quench more than one-half of the fluorescence of a dye with 1-ns lifetime.

By applying oxygen pressures up to 100 bar, Weber et al.[25] have extended the study of oxygen quenching to short lifetime probes in aqueous solutions (2–10 ns). It has been shown that indole ($\tau_0 = 4.1$ ns), tryptophan ($\tau_0 = 2.7$–2.9 ns), and tyrosine ($\tau_0 = 3.2$ ns) in aqueous solutions are quenched close to the diffusion-controlled value of 1.0×10^{10} M^{-1} s^{-1}. It has been concluded that every collision of oxygen with an excited free fluorophore in the solution is effective in quenching its potential fluorescence.

Oxygen under high pressure has been proved to be an ideal quencher in the study of excited states of biological molecules since unlike the more conventional quenchers iodide and Hg^{2+} it is nondestructive, reversible, and insensitive to charge effects caused by charged polyamino acids and to complexation by proteins.

The quenching of ethidium bromide, when intercalated into double helical DNA, is only $^1/_{30}$th as efficient as that of free dye in solution. This is ascribed to a reduced number of collisions with the dye. Other dyes
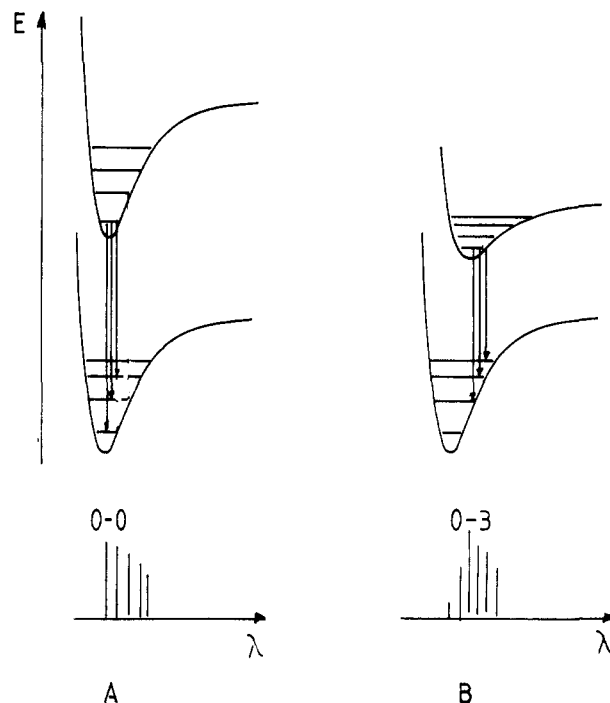

Figure 12. Schematic presentation of the oxygen quenching effect on the fluorescence in polar solvents: (A) short-lived emission directly after excitation before reorientation of solvent molecules; (B) long-lived emission after reorientation of solvent molecules.

bound to bovine serum albumin were also found to be relatively protected from the free diffusion of oxygen. Quenching of intrinsic or bound fluorophores by molecular oxygen is therefore an appropriate method for determining the accessibility of regions of the macromolecule surrounding the fluorophore.[25]

Oxygen quenching of tryptophan fluorescence in proteins has been used to obtain information on the dynamics of structural changes on the nanosecond time scale. The oxygen quenching constant (k_q) for a variety of proteins (e.g., human serum albumin, pepsin, ribonuclease) indicates that the apparent oxygen diffusion rate through the protein matrix is 20–50% of its diffusion rate in water. No tryptophan residues appear to be excluded from quenching, and no correlation of the fluorescence emission maxima with k_q was found, indicating that the oxygen diffusion is rapid in all regions of the protein, even in those regions which are normally considered to be inaccessible to the solvent. Obviously proteins undergo rapid structural fluctuations on the nanosecond time scale which permit diffusion of oxygen.[60]

Fluorophores in the excited state generally have an increased dipole moment relative to the ground state. Reorientation of polar groups surrounding the increased dipole moment is responsible for the red shifts of fluorescence emission spectra observed in polar solvents. A fraction of the excited molecules may emit before solvent relaxation is complete. Their fluorescence will thus appear at shorter wavelengths (see Figure 12). When a solution is quenched by oxygen, it is possible to observe selectively those molecules which emit rapidly after excitation, since these molecules are less likely to collide with oxygen and be quenched. Oxygen quenching thus provides a method by which relaxation effects in fluid media can be studied. A sufficiently high oxygen concentration may decrease the fluorescence

lifetime to a point such that it becomes comparable with or even shorter than the relaxation time of the reorientation process of the solvent molecules. In fluid solvents with viscosities of about 1 cP, τ_R is of the order of 10^{-11} s.

Weber et al. have demonstrated that under strong oxygen quenching it is possible to determine the fluorescence spectral distribution in the first few picoseconds after excitation. Quenching by oxygen under a pressure of 100 bar reduces the fluorescence lifetime of ethanolic solutions of 1-anilinonaphthalene-8-sulfonate or indole to 54 and 36 ps, respectively. The unquenched values are 13.4 and 5.0 ns. The corresponding fluorescence maxima are blue-shifted by 5 and 8 nm, respectively. Thus one can say that the quenching technique provides a 100-fold improvement in time resolution of fluorescence.[61]

The method of strong fluorescence quenching by oxygen proved similarly useful in analyzing the dual fluorescence spectrum of 4-(dimethylamino)benzonitriles[26] and p-(dimethylamino)acetophenone.[62] The low-energy fluorescence band of 2-methyl-4-(dimethylamino)benzonitrile (eq 11) (a, ca. 20600 cm^{-1})

(11)
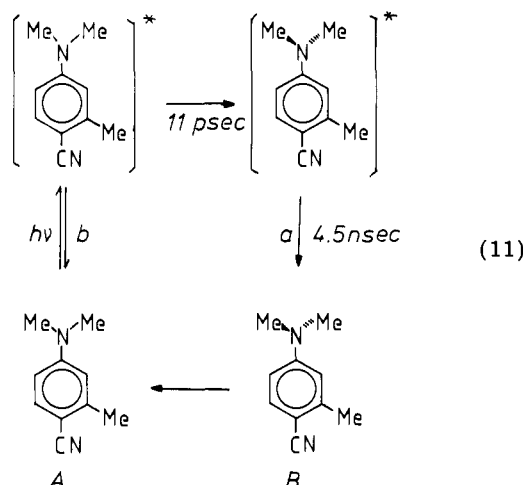
is quenched much more readily than the high-energy band (b, ca. 27800 cm^{-1}), e.g., by factors of 191 and 1.6, respectively, in presence of about 0.78 M oxygen (= 98 bar). This means that both fluorescences differ considerably in their lifetimes, where the fluorescence b predominates a short time after excitation. The higher energy fluorescence b is assigned to a planar isomer B, the lower energy emission a to the isomer A with a twisted amino group. It was derived from the measurements that the isomerization B* → A* occurs with a lifetime of 11 ps whereas the solvent orientation time in this case is only 1 ps. The lifetime of A* is 4.5 ns.[26] Analogous results were obtained for p-(dimethylamino)acetophenone.[62]

F. Trapping of Short-Lived Intermediates by Oxygen

Oxygen can be used as a trapping agent for photochemically generated transient species. The trapping of triplet biradicals usually leads to peroxides. Triplet biradicals with an unusual long life such as trimethylenemethane are already trapped at 1 atm of oxygen pressure. For intermediates with shorter lifetimes, high pressures of oxygen (= higher concentrations) are necessary.

When compound 7 was irradiated with the ultraviolet lines of an argon ion laser (351.1 and 363.7 nm) under medium oxygen pressure (5.5 to 10.5 bar), a complete suppression of the dimeric hydrocarbon product usually obtained was observed. Instead the peroxide 8 is formed. Formation of the bridged peroxide 9 was not observed (eq 12).[14]


(12)
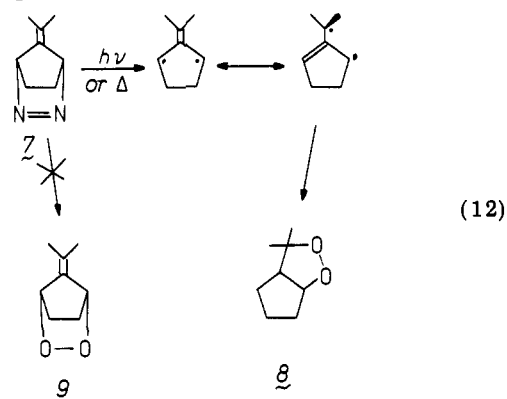
Clark and Steel[63] observed quenching of the hydrocarbon products on photolysis of azo compound 10 (eq 13) and speculated that this was due to the trapping

(13)
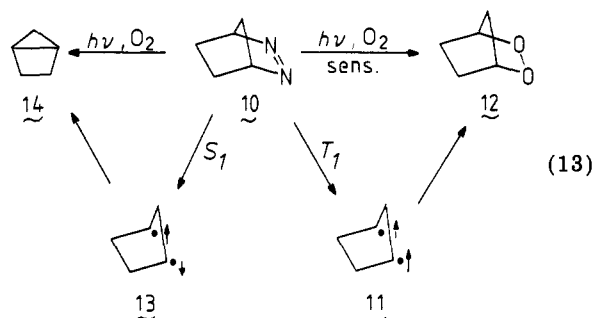
of a biradical intermediate by oxygen. They did not report any isolation of product arising from this trapping process. Upon the benzophenone-sensitized photodecomposition of 10, Wilson and Geiser[14] were able to identify the peroxide 12. The latter is produced when the intermediate triplet biradical 11 is trapped under 10 bar of oxygen. Direct irradiation of 10 produces the singlet biradical 13 which collapses to bicyclo[2.1.0]pentane 14 before it can be trapped by oxygen. Careful attention must be devoted to the experimental conditions. The optimum oxygen pressures seem to be about 10 bar. At oxygen pressures higher than about 15 bar, the oxygen quenching of benzophenone triplets dominates to the extent that no reaction occurs.[14] Population of the triplet state of 10 by direct $S_0 \rightarrow T_1$ excitation under 50 bar of oxygen also yields products which show a positive peroxide test, probably due to formation of 12.[51]

Oxygen trapping of the biradical 16 derived from 15 affords the bicyclic peroxides 18 and related hydroperoxides (eq 14). These hydroperoxides appear to

(14)
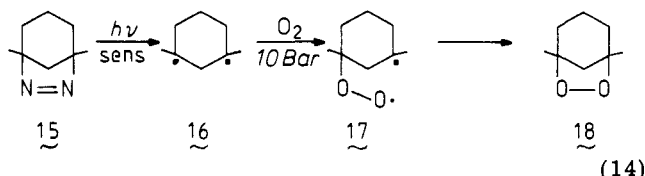
arise from a stepwise trapping of the biradical 16 in which the intermediate peroxy biradical 17 can undergo

intramolecular hydrogen abstraction as well as cyclization to 18.

The sensitized decomposition of the vinylazoalkane 19 (eq 15) is extremely temperature dependent. The

$$(15)$$

$$\underset{19}{\sim} \qquad \underset{20}{\sim} \qquad \underset{21}{\sim}$$
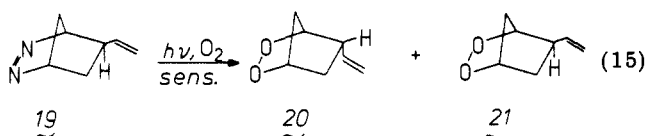
peroxide yield is greatly reduced at lower temperatures, apparently due to the trapping of intermediates in which only one carbon–nitrogen bond has been cleaved. The peroxide yield passes through an optimum value and decreases at higher temperature due to peroxide decomposition. The endo- and exoperoxides 20 and 21 are obtained in about equal yield.[64a] Further examples of oxygen trapping, e.g., reactions of quinone with olefins and oxygen, which give trioxenes, will be published.[64b]

The strongly forbidden $S_0 \rightarrow T_1$ absorption (λ 2900–3400 Å) of benzene is enhanced at high oxygen concentrations (cf. section IIIB). When benzene samples are saturated with oxygen under a pressure of 100 bar and irradiated with ultraviolet light of the spectral range 2900–3600 Å, a reaction takes place. The products phenol ($\phi \approx 0.03$) and o-benzoquinone are identified (eq 16 and 17). It was established that these

$$(16)$$

$$(17)$$
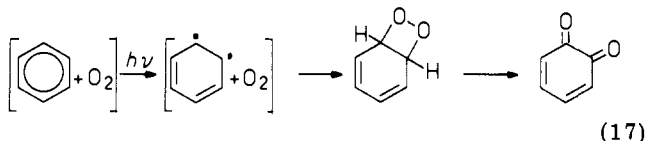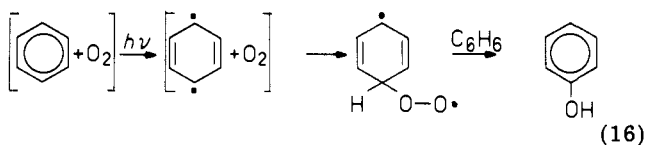
products are formed via benzene excited to its biradical-like triplet state and oxygen in its ground state.[65,66]

Latourette[29] describes the photooxidation of xylenes and toluenes to hydroperoxides at 200 bar oxygen pressure in benzene solution (eq 18–20).

$$(18)$$

$$(19)$$

$$(20)$$
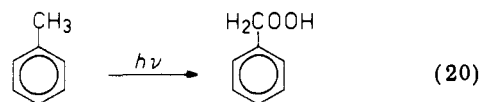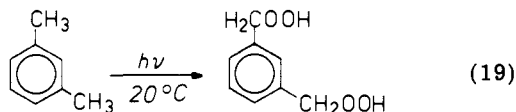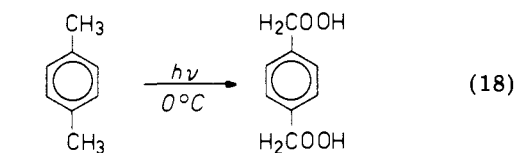
IV. High Pressure of Hydrogen

A. Hydrogen Solubility

At small partial pressures of solute the solubility of gases usually decreases with increasing temperature, reaches a minimum, and may increase again at relatively high temperatures. This general rule is not
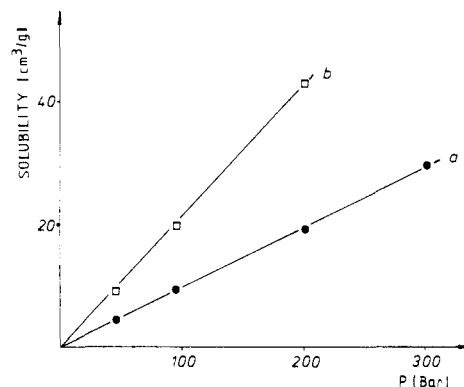
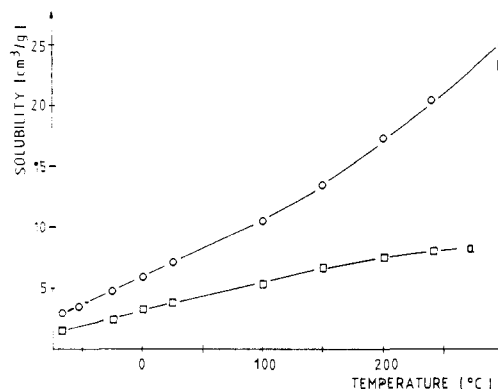Figure 13. Solubility of hydrogen in cyclohexane:[37a] (a) at 25 °C; (b) at 150 °C.

Figure 14. Solubility of hydrogen in toluene:[37a] (a) 50-bar H$_2$ pressure; (b) 100-bar H$_2$ pressure.

obeyed for high pressures of light gases. Notably the behavior of hydrogen is completely different in that it already shows a pronounced positive temperature coefficient at ambient temperatures. Figure 13 shows that the solubility of hydrogen decreases with increasing temperature, but it is increased with increasing pressure, as shown in Figure 14.[37a]

B. Photochemical Hydrogenations

The photochemical hydrogenations at elevated hydrogen pressures described so far in the literature use coordination compounds of transition metals as catalysts. They belong to the class of homogeneous as opposed to heterogeneous hydrogenations, which means that the catalyst and the substrate are both homogeneously dissolved in the liquid phase. The systems consist of two phases, of course. The liquid phase contains the substrate to be hydrogenated, the catalyst, and a certain amount of dissolved hydrogen. The gas phase contains the bulk of the hydrogen. Since only the dissolved hydrogen can take part in the reaction, it is necessary to mix gas and liquid phases, otherwise the equilibration of the hydrogen between the two phases is rate determining and leads to erroneous results in the quantitative measurements.

The homogeneous hydrogenation of 1,3-cyclohexadiene (eq 21) to cyclohexene with IrClCO(PPh$_3$)$_2$

$$(21)$$
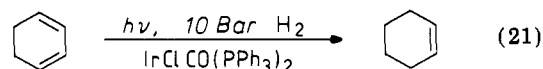
as catalyst is a photoinduced reaction of high selectivity. At 70 °C, a hydrogen pressure of 10 bar, and a ratio of substrate to catalyst of 100 000:1, the mean catalytic
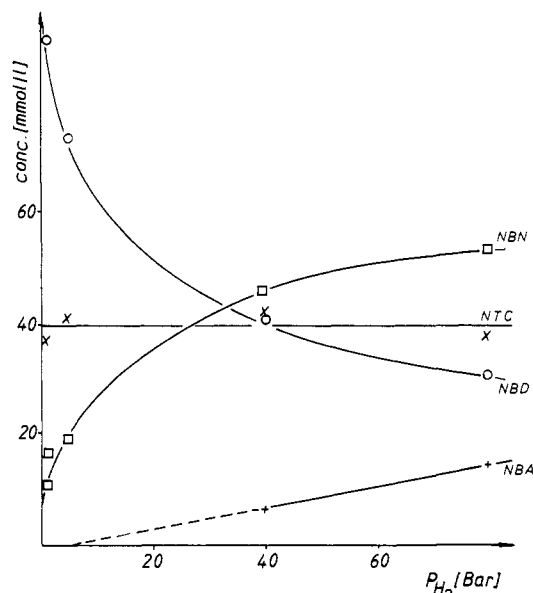
Figure 15. Influence of H_2 pressure on the photochemical hydrogenation of norbornadiene catalyzed by $Cr(CO)_6$.[71,72] NBN = norbornene, NTC = nortricyclene, NBD = norbornadiene, NBA = norbornane. Conditions: 25 °C, 125-W medium-pressure Hg lamp, 0.0036 M $Cr(CO)_6$, 0.14 M NBD in n-decane.

activity is 196 mol product per mol of catalyst per min and the turnover number is 96 260 mol of product per mol of catalyst. Only 10 min of irradiation is necessary to activate the catalyst, probably by one or both of the following reactions (eq 22 and 23).[11] With $Cr(CO)_6$ as

$$IrClCO(PPh_3)_2 \xrightarrow{h\nu} IrClCOPPh_3 + PPh_3 \quad (22)$$

$$IrClCO(PPh_3)_2 \xrightarrow{h\nu} IrCl(PPh_3)_2 + CO \quad (23)$$

the catalyst it is possible to hydrogenate dienes photochemically to monoenes already at room temperature and normal pressure.[67,68] An increase in hydrogen pressure accelerates the reaction significantly without affecting the selectivity, i.e., no cyclohexane is formed even at 90 bar.[69]

The photochemical hydrogenation of norbornadiene (NBD) with $Cr(CO)_6$ or $Cr(NBD)(CO)_4$ as catalyst yields nortricyclene and norbornene in a ratio of ~3:1 at normal pressure (eq 24).[70] Under a hydrogen

$$(24)$$
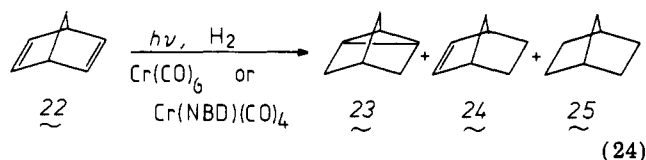
pressure of 100 bar the reaction proceeds much faster than at normal pressure and yields in addition to **23** and **24** a significant amount of norbornane **25**. Figure 15 shows that this increase of the reaction rate is mainly caused by an increased formation of **24** and **25**, whereas the formation rate of **23** is almost independent of pressure. As a consequence of the different reaction orders with respect to hydrogen, the nortricyclene to norbornene ratio becomes 0.8:1 at 100 bar of hydrogen pressure.[71,72]

C. Organometallic Reactions

Krusic has developed a technique to measure ESR spectra of photochemically produced paramagnetic
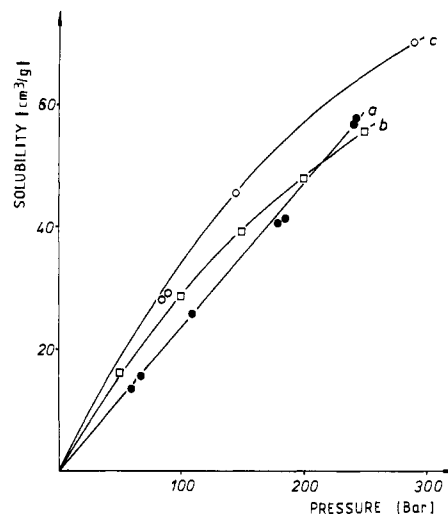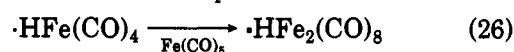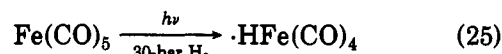

Figure 16. Solubility of carbon monoxide in methanol:[37b] (a) 25 °C; (b) 90 °C; (c) 140 °C.

species under high pressures.[12,13] At about 30-bar hydrogen pressure, $Fe(CO)_5$ was found to form the paramagnetic carbonyl hydride $HFe_2(CO)_8$, probably via the mononuclear analogue $HFe(CO)_4$ (eq 25 and 26).

$$Fe(CO)_5 \xrightarrow[\text{30-bar } H_2]{h\nu} \cdot HFe(CO)_4 \quad (25)$$

$$\cdot HFe(CO)_4 \xrightarrow{Fe(CO)_5} \cdot HFe_2(CO)_8 \quad (26)$$

V. High Pressure of Carbon Monoxide

A. Carbon Monoxide Solubility

At room temperature the solubility of CO increases linearly with pressure in most organic solvents. At higher temperatures, however, irregularities occur, as can be seen from Figure 16, showing the solubility of CO in methanol,[37b] which is of practical importance.

B. Reactions with Carbon Monoxide

The reaction of carbon monoxide and methanol with olefins catalyzed by transition-metal carbonyls is known as hydroesterification and represents a convenient route to carboxylic acid esters. UV irradiation was found to enhance the formation of the active catalyst (probably $HCo(CO)_4$) from cobalt acetate (eq 27).[73] At 80 °C and
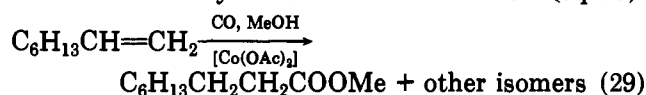
$$Co(OAc)_2 \cdot 4H_2O \xrightarrow[\text{CO, MeOH}]{h\nu} HCo(CO)_4 \quad (27)$$
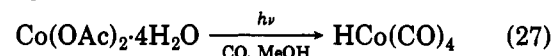
a CO pressure of 85 bar, the hydroesterification of cyclohexene (eq 28) was enhanced by UV light throughout

$$(28)$$
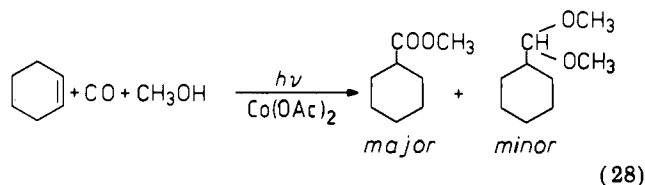
the reaction, but was slowed down when the irradiation was interrupted (Figure 17a).

1-Octene, however, exhibits a different behavior under irradiation. In this case UV light is only necessary to initiate the hydroesterification reaction (eq 29).
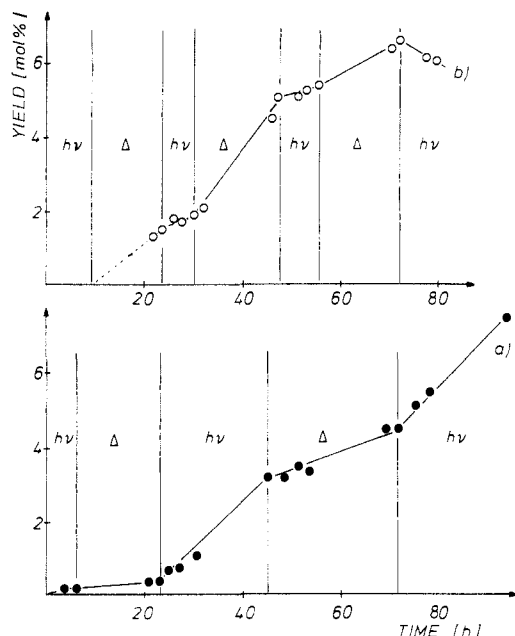
$$C_6H_{13}CH{=}CH_2 \xrightarrow[\text{[Co(OAc)}_2]]{\text{CO, MeOH}}$$

$$C_6H_{13}CH_2CH_2COOMe + \text{other isomers} \quad (29)$$

Figure 17. Photochemical hydroesterification of cyclohexene (a) and 1-octene (b).[73] (a) Methyl cyclohexanecarboxylate; (b) methyl nonanoate. $h\nu$ = irradiation periods, Δ = dark periods. Conditions: 80 °C, 80-bar CO, 600-W medium-pressure Hg lamp, Pyrex filter, 3.3 M olefin, 0.0057 M Co(OAc)$_2$·4H$_2$O in methanol.

Once the reaction is started, further irradiation inhibits the thermal hydroesterification, as can be seen from curve b in Figure 17.

The reasons for the differences between cyclohexene and 1-octene are not clear, but similar processes as described for the hydroformylation (see section VIB) might play a role.[73]

When a pentane solution of diazabicyclo[2.2.1]heptene **26** is irradiated in the presence of 80 bar of CO, the colorless solution turns deep yellow, and IR evidence for the formation of a di- or polyketone is obtained. Since this effect is not observed without irradiation or in the absence of CO, a trapping of the primarily formed biradical **27** by carbon monoxide seems likely, although the diketone **28** was not clearly identified.[74] Nevertheless eq 30 represents an analogous process using molecular oxygen (cf. eq 15, section IIIF).

(30)
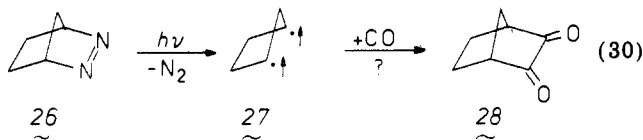
VI. High Pressure of Synthesis Gas

A. Synthesis Gas Solubility

A mixture of carbon monoxide and hydrogen is usually termed synthesis gas, which is of enormous importance for a number of chemical reactions starting with C$_1$-building blocks, such as hydroformylation or Fischer–Tropsch synthesis.

The examples of solubility diagrams in Figure 18 show that CO is more soluble than H$_2$, which displays an irregular behavior with increase in temperature.[37c] Thus the concentration of the dissolved gases could be different to that which would be concluded from a consideration of the composition of the gas phase only. Caution is therefore necessary when equating gas
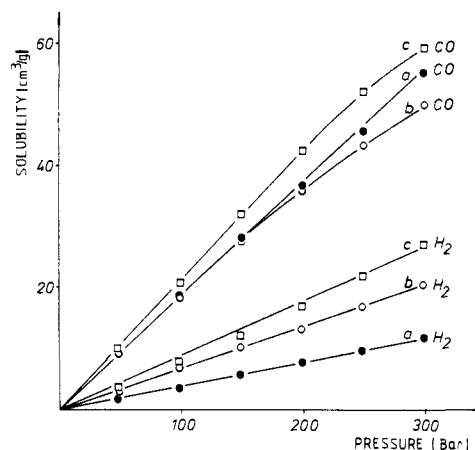

Figure 18. Solubility of synthesis gas CO/H$_2$ in methanol:[37c] (a) 30 °C; (b) 90 °C; (c) 140 °C. Gas-phase composition: (a) 27 mol % H$_2$; (b, c) 31.3 mol % H$_2$.

pressure with the concentration of gaseous components in the liquid.
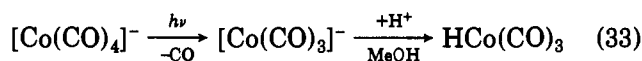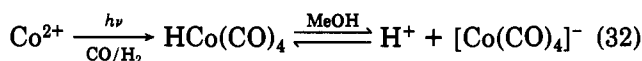
B. Photochemical Hydroformylation

The hydroformylation reaction is of industrial importance for the production of aldehydes from olefins (eq 31). It is usually carried out at elevated tempera-
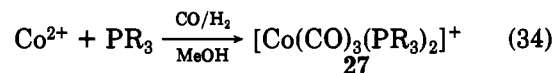
$$RCH\!=\!CH_2 \xrightarrow[\text{[catal.]}]{\text{CO/H}_2} RCH_2\text{-}CH_2CHO + R\text{-}CH(CH_3)CHO \quad (31)$$
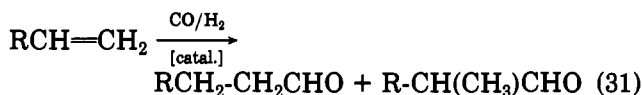
tures and pressures: 140–170 °C, 200–300 bar with cobalt catalysts and 100–120 °C, 20–50 bar with rhodium catalysts.[75]

Irradiation with UV light allows the reaction to run under very mild conditions. Very high selectivities of straight-chain products, which are usually more valuable, are obtained with Co/PPh$_3$ catalysts. Propene and 1-octene are converted to aldehydes which are respectively 99% and 90% linear (Table IV). Positive radiation effects are observed in methanol solvent and with ionic catalysts such as Co(OAc)$_2$, RhCl$_3$, etc.[76-78]

Two different processes were found under investigation to be responsible for the observed light effect. The first is a photochemically initiated reduction of the metal salts to low-valent metal carbonyls (eq 32) and the second is an activation of the cobalt tetracarbonyl anion to give the active catlayst HCo(CO)$_3$ (eq 33). In

$$Co^{2+} \xrightarrow[\text{CO/H}_2]{h\nu} HCo(CO)_4 \xrightleftharpoons{\text{MeOH}} H^+ + [Co(CO)_4]^- \quad (32)$$

$$[Co(CO)_4]^- \xrightarrow[\text{-CO}]{h\nu} [Co(CO)_3]^- \xrightarrow[\text{MeOH}]{+H^+} HCo(CO)_3 \quad (33)$$

the presence of phosphine the cation **27** is formed immediately when cobalt acetate in methanol is pressurized with 80 bar of synthesis gas (eq 34). The cation

$$Co^{2+} + PR_3 \xrightarrow[\text{MeOH}]{\text{CO/H}_2} [Co(CO)_3(PR_3)_2]^+ \quad (34)$$
$$\phantom{Co^{2+} + PR_3 \xrightarrow[\text{MeOH}]{\text{CO/H}_2} }\mathbf{27}$$

27 is the photoactive species and is converted to the hydroformylation catalyst **28** upon irradiation (eq 35).[36,79]

$$[Co(CO)_3(PR_3)_2]^+ \xrightarrow{h\nu} HCo(CO)_3PR_3 \quad (35)$$
$$\phantom{[Co(CO)_3(PR_3)_2]^+ \xrightarrow{h\nu} }\mathbf{28}$$
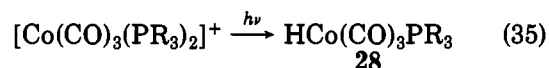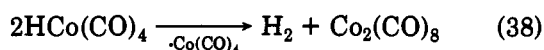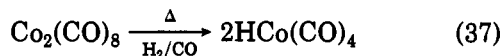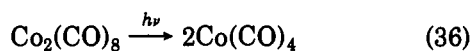
TABLE IV. Photochemical Hydroformylation of Olefins and Dienes with CO/H$_2$[a]

entry	starting material	catalyst	T, °C	t, h	main product, selectivity, mol % (conversion, mol %)
1	propene[b,c,l,n]	Co(OAc)$_2$/P(n-Bu)$_3$ (1:10)	85	30	n-butyraldehyde, 99 (20)
2	propene[d,l,n]	Co$_2$(CO)$_8$	60	26	n-butyraldehyde + acetal, 65 (25)
3	1-octene[b,l,n]	Co(OAc)$_2$/P(n-Bu)$_3$ (1:10)	85	26	n-nonanal, 90 (46)
4	1-octene[b,l,n]	Co$_2$(CO)$_8$/P(n-Bu)$_3$ (1:20)	85	28	n-nonanal, 87 (50)
5	1-octene[b,l,n]	Co(OAc)$_2$	85	6	n-nonanal + acetal, 68 (80)
6	1-octene[b,m]	RhCl$_3$·3H$_2$O/PPh$_3$	20	17	C$_9$ acetals, 14.2 (3.51)
7	1-octene[m]	RhHCO(PPh$_3$)$_3$	20	17	C$_9$ aldehydes, 46 (14.6) Δ = 77.8 (4.5)
8	1-octene[b,m,p]	Fe(CO)$_5$[e]	85	15.5	C$_9$ aldehydes, 39.4 C$_8$ alcohols, 60.6 (31.7)
9	4-octene[b,m]	Co$_2$(CO)$_8$	80	2	C$_9$ acetals, 85.2 (17)
10	cyclohexene[l]	Co(OAc)$_2$	85	12	cyclohexanecarbaldehyde + acetal, >95 (13)[f]
11	styrene[m]	RhHCO(PPh$_3$)$_3$/PPh$_3$ (1:5)	20	17	ethylbenzene, 57, Δ = 7.9 2-phenylpropanal, 38, Δ = 90.8 3-phenylpropanal, 5.0, Δ = 1.3 (39.6, Δ = 2.3)
12	styrene[l]	Co(OAc)$_2$/PPh$_3$ (1:10)	80		ethylbenzene, Δ = 3-phenylpropanal
13	butadiene[d,m]	Co$_2$(CO)$_8$	85	22	aldehydes + acetals, 82.3 (42.5)
14	isoprene[b,m]	Co(OAc)$_2$/P(n-Bu)$_3$ (1:4.5)	80	36	unsaturated monomeric oxo products, 2.0 oxo products of dimers, 3.6 unsaturated linear dimers, 6.2[g]
15	1,5-hexadiene[b,m]	Co$_2$(CO)$_8$	80	5	monoaldehydes, 67 bisaldehydes, 8.3 (60)[g]
16	1,5-hexadiene[m]	RhHCO(PPh$_3$)$_3$	80	16	monoaldehydes, 39.4, Δ = 90.9 isomerization, 60.6, Δ = 9.1 (66, Δ = 11)
17	2,4-hexadiene[h,m]	Co$_2$(CO)$_8$	80	15	monoaldehydes, 65.6 isomerization, 34.3 (99)[g]
18	2,4-hexadiene[h,m]	Co(OAc)$_2$	80	15	monoaldehydes, 20; isomerization, 53.3 (75)[g]
19	2,4-hexadiene[b,m]	RhHCO(PPh$_3$)$_3$	80	17.5	isomerization, >95 (57)[g]
20	norbornadiene[b,l]	RhCl$_3$·3H$_2$O	25	18	A, 10; B, 90 (99)[i]
21	norbornadiene[b,l]	RhCl$_3$ + PPh$_3$[k] (1:10)	25	5.5	A, 10; B, 90 (75)[i]
22	norbornadiene[b,l]	RhHCO(PPh$_3$)$_3$	25	4	A, 20; B, 80 (80)[i]

^{a} CO/H$_2$ = 1/1, solvent methanol, irradiation with a high-pressure mercury lamp through Pyrex. ^{b} No reaction without irradiation. ^{c} 85 bar. ^{d} Reaction rate is the same with or without irradiation. ^{e} Solvent THF. ^{f} 30 h of thermal reaction affords 7% cyclohexanecarbaldehyde and acetal. ^{g} Weight %. ^{h} 22% polymers, 3% isomerization. ^{i} A = 5-norbornene-2-carbaldehyde, B = bishydroformylation products. ^{k} 100 bar. ^{l} Reference 76. ^{m} Reference 73. ^{n} Reference 36. ^{p} Hydroformylation of 1-hexene and propene with Fe(CO)$_5$, Fe(CO)$_5$/Co$_2$(CO)$_8$, and Ru$_3$(CO)$_{12}$ was investigated by Krusic,[81] but details are to be published.

The reaction is inhibited by UV light under normal hydroformylation conditions and with Co$_2$(CO)$_8$ as catalyst in hydrocarbon solvents. The retarding effect has been found to be due to the photodissociation of Co$_2$(CO)$_8$. The formed Co(CO)$_4$ radicals catalyze the decomposition of the active catalyst HCo(CO)$_4$ which is formed in a thermal reaction between Co$_2$(CO)$_8$ and H$_2$ (eq 36–38).[34,79]

$$Co_2(CO)_8 \xrightarrow{h\nu} 2Co(CO)_4 \qquad (36)$$

$$Co_2(CO)_8 \xrightarrow[H_2/CO]{\Delta} 2HCo(CO)_4 \qquad (37)$$

$$2HCo(CO)_4 \xrightarrow{\cdot Co(CO)_4} H_2 + Co_2(CO)_8 \qquad (38)$$

Further examples for the hydroformylation of dienes and with rhodium catalysts are listed in Table IV. To date no mechanistic details are known about the photocatalytic reactions with rhodium compounds, but similar mechanistic considerations as those for cobalt may be valid.

An interesting example is the photochemical hydroformylation with Fe(CO)$_5$, which is thermally a very poor catalyst.[73,80,81] Paramagnetic carbonylferrates might be intermediates in this reaction.[81]

VII. High Pressure of Ethylene

A. Ethylene Solubility

Ethylene is an ideal building block in organic synthesis. It is cheap, readily available, and fairly reactive
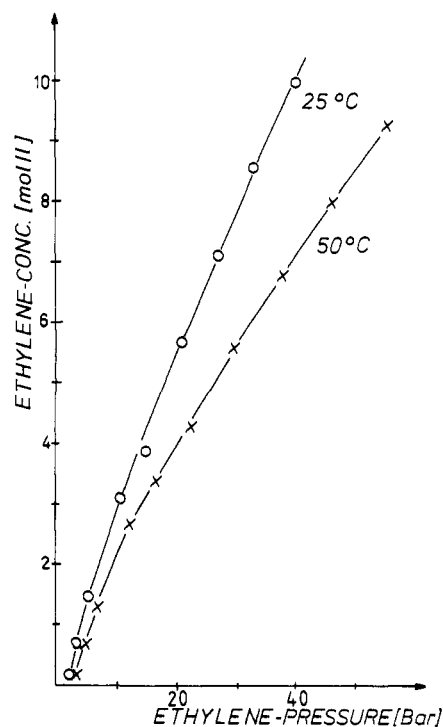

Figure 19. Solubility of ethylene in CH$_2$Cl$_2$.[82]

toward addition reactions. Another important feature is its unique solubility in organic solvents at high pressures. In CH$_2$Cl$_2$, for instance, the concentration of ethylene is ca. 12 mol/L at 50 bar and 25 °C (Figure 19). This is a concentration comparable only to neat

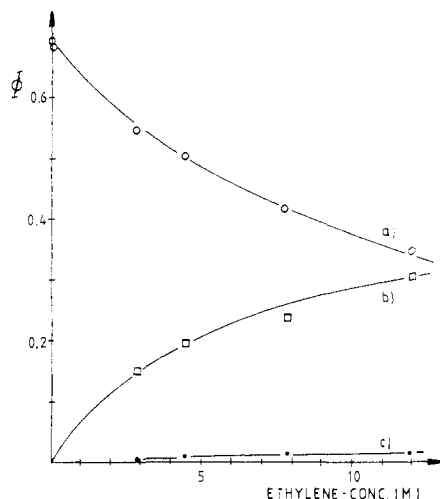**Figure 20.** Photochemical 2 + 2 cycloaddition of 1,3-cyclo-hexadiene and ethylene at elevated pressure (12 M = 55-bar ethylene).[83] (a) Quantum yield of cyclohexadiene dimers; (b) quantum yield of cis-bicyclo[4.2.0]oct-2-ene; (c) quantum yield of unidentified isomers. Conditions: 125-W medium-pressure Hg lamp, Pyrex filter, 0.25 M cyclohexadiene, 0.05 M 2-acetyl-naphthalene in CH_2Cl_2, $T = 25$ °C.

liquid olefins. Pressures higher than 50 bar do not increase the solubility further, at least not at room temperature, since ethylene has a relatively low critical point ($T = 9.5$ °C, $P = 50.76$ bar).[82] These features make ethylene a particularly interesting candidate for photochemical studies under pressure.

B. Cycloaddition Reactions

The photochemical 1,2-addition of olefins to 1,3-cyclohexadiene is only possible with an ~10-fold excess of the olefin, since the dimerization of the diene is a very efficient process and would otherwise dominate. Consequently the [2 + 2] cycloaddition of ethylene to 1,3-cyclohexadiene could only be observed at pressures >10 bar in CH_2Cl_2 (eq 39). The quantum yield for the
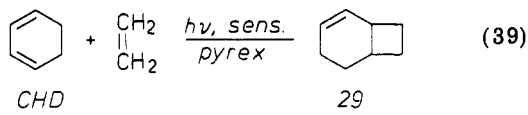
1-acetylnaphthalene-sensitized formation of cis-bicy-clo[4.2.0]oct-2-ene (**29**) increases with ethylene pressure, and the dimer formation is simultaneously depressed, as shown in Figure 20.[83] A similar effect is observed for the methyl esters of maleic and fumaric acids. Due to the fast cis–trans isomerization, no cycloaddition reaction is observed at 1 bar of ethylene, but with increasing pressure cyclobutane-1,2-dicarboxylic acid ester is also formed (eq 40, 41). Predominantly the trans

R= $-COOCH_3$, $-CN$
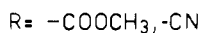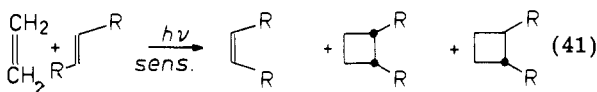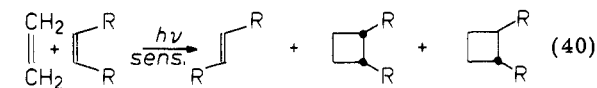
isomer is formed (~80%). The quantum yields for the cycloadducts, however, remain low even at 60 bar of ethylene ($\phi \sim 10^{-3}$ to 10^{-4} as compared to $\phi = 0.2$ for

TABLE V. Examples of Photochemical Telomerization Reactions with Ethylene at Elevated Pressure

| telogen	products	ref
$HCONH_2$	$CH_3CH_2(CH_2CH_2)_{n-1}CONH_2$	87
$HCONMe_2$	$CH_3CH_2(CH_2CH_2)_{n-1}CONMe_2$ + $HCON(Me)CH_2(CH_2CH_2)_{n-1}CH_2CH_3$	88
		89

the cis–trans isomerization).

In contrast to the results with maleic and fumaric esters it has been found that the quantum yield for the cycloaddition of ethylene to maleic anhydride is decreased with increasing ethylene pressure, due to a simultaneous quenching process.[24]

The addition of photoexcited benzene to olefins can give either 1,2, 1,3, or 1,4 adducts, depending on the nature of the olefin. It has been found that ethylene adds to S_1 benzene in the meta position and that the 1,3-adduct **30** is the major product (eq 42). The
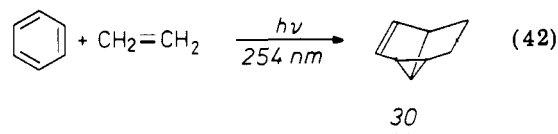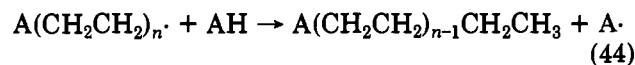

quantum yield for product formation is directly dependent upon olefin pressure. Values of $\phi = 0.1$ were obtained at 50 bar of ethylene. The major side products are the 1,2-adduct **31** and its tautomer **32**, which at
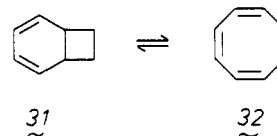
higher conversions undergo further photoreactions. The preference of the 1,3 adduct shows that the electron affinities, and not the ionization potentials as previously stated,[84] are important to predict the addition mode. With an electron affinity of -1.8 eV ethylene is a poor electron donor and with an ionization potential of 10.5 eV also a poor electron acceptor. These are the typical conditions for a meta addition to benzene.[85,86]
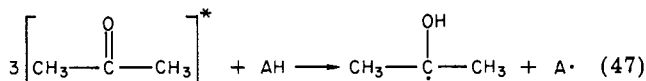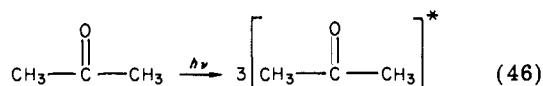
C. Free-Radical Reactions

High-pressure photochemistry has been used to initiate free-radical reactions of ethylene, such as telomerization and polymerization. The telomerization reaction starts with the formation of a telogen radical, A·, which adds to ethylene monomers (eq 43) until the radical terminates by hydrogen abstraction (eq 44) or some other process (eq 45). Examples for photoin-

$$A\cdot + nCH_2{=}CH_2 \rightarrow A(CH_2CH_2)_n\cdot \qquad (43)$$

$$A(CH_2CH_2)_n\cdot + AH \rightarrow A(CH_2CH_2)_{n-1}CH_2CH_3 + A\cdot \qquad (44)$$

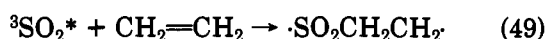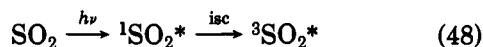$$2A\cdot \rightarrow A{-}A \qquad (45)$$

duced telomerizations are summarized in Table V. The number of ethylene units in the product molecules range from 1 to 20 in a geometrical distribution. With increasing ethylene pressure the amount of products containing more than one ethylene unit increases, which is the desired effect when the reaction is used to synthesise raw materials for detergents. The telomeriza-

tions are usually initiated by hydrogen abstraction of photoexcited ketones, notably acetone (eq 46, 47).

$$CH_3-\overset{O}{\overset{\|}{C}}-CH_3 \xrightarrow{h\nu} {}^3\left[CH_3-\overset{O}{\overset{\|}{C}}-CH_3\right]^* \quad (46)$$

$${}^3\left[CH_3-\overset{O}{\overset{\|}{C}}-CH_3\right]^* + AH \longrightarrow CH_3-\overset{OH}{\overset{|}{C}}-CH_3 + A\cdot \quad (47)$$

When a mixture of sulfur dioxide and ethylene in cyclohexane solvent is irradiated with a medium-pressure Hg lamp, poly(ethylene sulfone) is formed in high yield. The product is an alternating copolymer containing SO_2 and ethylene units in a molar ratio of 1:1 which is thermally very stable and very pure, since it is not polluted by chemical starters. The reaction is thought to be initiated by photoexcited sulfur dioxide which adds to ethylene (eq 48, 49).[90]

$$SO_2 \xrightarrow{h\nu} {}^1SO_2{}^* \xrightarrow{isc} {}^3SO_2{}^* \quad (48)$$

$${}^3SO_2{}^* + CH_2{=}CH_2 \rightarrow \cdot SO_2CH_2CH_2\cdot \quad (49)$$

VIII. High Pressure of Other Gases

A. Xenon

Under a high pressure of xenon (143 bar = 2.3 M in α-chloronaphthalene) the intensity of the spin-forbidden $S_0 \rightarrow T_1$ transition of α-chloronaphthalene is enhanced to a degree that it can be observed in the UV spectrum. The most probable explanation of the observed phenomenon is an intermolecular heavy atom effect.[91] The perturbating strength of Xe is found to be smaller than that of oxygen by about three orders of magnitudes and ten times smaller than that of ethyl iodide. It has, however, the advantage of almost total chemical inertness, which could be an advantage in studying the triplet levels of reactive molecules.

Calcaterra and Schuster[92] report a heavy atom effect on the reaction of β,γ-unsaturated ketone **33** (eq 50)


$$(50)$$
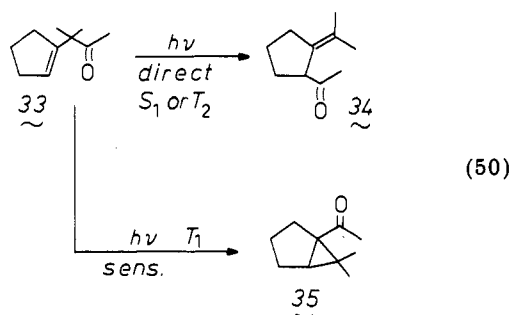
induced by 2.2 bar of xenon. They found that the quantum yield for the formation of **34** upon direct irradiation was increased by 20% and that the fluorescence quantum yield of **33** was decreased by 20%. They ascribe the observed effect to an enhanced intersystem crossing, $S_1 \rightarrow T_2$, caused by an external heavy atom effect of the xenon. This is unusual insofar as the heavy atom effects on ketones which possess lowest n,π* states are not expected[38] and that the reaction occurs from the T_2 state, thus violating the "El-Sayed rule". On the other hand reactions from the T_2 state, which is actually the first excited state of a separate chromophore of β,γ-unsaturated ketones, have been reported previously.[93-95] We find it very surprising, however, that such

a small xenon pressure (2.2 bar ≤ 0.1 M) should be sufficient to cause a measurable heavy atom effect on an n,π* singlet state with such a short lifetime as **33** (τ = 0.41 ns).

B. Propene

The cycloaddition of propene to S_1-excited benzene under a pressure of 15 bar leads to the endo- and exo-1,3 adducts **36** and **37** (eq 51).[85] Compared to ethylene (see

$$(51)$$
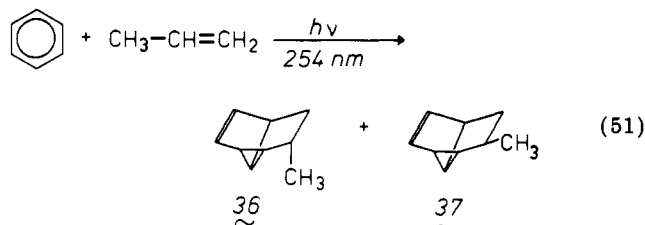
section VIIB) the addition of propene to benzene is rather a clean reaction. Except for a small amount of polymer, no side products were formed.
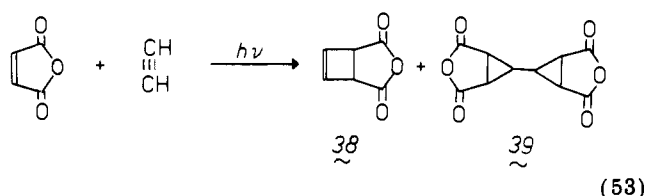
C. Acetylene

Acetylene has been studied in photocycloadditions with 1,3-cyclohexadiene and maleic anhydride. With cyclohexadiene the 1,2- and 1,4-cycloaddition products are formed at 15 bar of acetylene pressure (eq 52). At

$$(52)$$
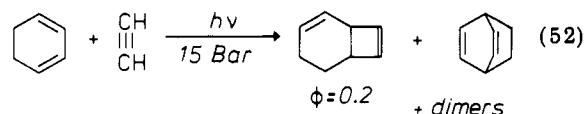
normal pressure dimerization of cyclohexadiene only is observed.[83]

Acetylene reacts with maleic anhydride in CH_2Cl_2 to form cyclobutenecarboxylic acid anhydride (**38**), which is an interesting monomer for polyesters. Its yield increases with pressure from ϕ = 0.003 at 5 bar to ϕ = 0.022 at 17 bar of acetylene, due to the increased solubility (eq 53).[24] A similar effect has been observed

$$(53)$$

upon lowering the temperature at normal pressure. At low acetylene concentrations (e.g., 1 bar, room temperature), the double adduct **39** is the major product.[96]

IX. References

(1) Brauer, H.-D.; Schmidt, R.; Kelm, H. In "High Pressure Chemistry"; Kelm, H., Ed.; D. Reidel: Dordrecht, 1978; pp 521–567.
(2) Drickamer, H. G.; Frank, C. W. "Electronic Transitions and the High Pressure Chemistry and Physics of Solids"; Chapman and Hall: London, 1973.
(3) Offen, H. W. In "Organic Molecular Photophysics"; Birks, J. B., Ed.; Wiley: London, 1973; Vol. 1.
(4) Oksengorn, B.; Vu, H.; Vodar, B. "Physics of High Pressures and the Condensed Phase"; van Itterbeek, A., Ed.; Wiley: London, 1965.
(5) Weigang, O. E., Jr.; Robertson, W. W. In "High Pressure Physics and Chemistry"; Bradley, R. S., Ed.; Academic Press: New York, 1963; Vol. 1, pp 177–206.
(6) Stanley, E. B., Jr.; Robertson, W. W. In "High Pressure Physics and Chemistry"; Bradley, R. S., Ed.; Academic Press:

New York, 1963; Vol. 1, pp 376–409.
(7) Palmer, D. A.; Kelm, H. *Coord. Chem. Rev.* **1981**, *36*, 89–153.
(8) Asano, T.; Le Noble, W. J. *Chem. Rev.* **1978**, *78*, 407.
(9) (a) Luther, K.; Troe, J. *Chem. Phys. Lett.* **1974**, *24*, 85. (b) Chervinsky, S.; Oref, I. *J. Phys. Chem.* **1977**, *81*, 1967.
(10) Strohmeier, W.; Kaiser, A. *J. Organomet. Chem.* **1976**, *114*, 273.
(11) Strohmeier, W.; Steigerwald, H. *J. Organomet. Chem.* **1977**, *125*, C37–C39.
(12) Krusic, P. 2nd International Symposium on Homogeneous Catalysis, Düsseldorf, 1980, Abstracts of Papers, p 68.
(13) Krusic, P. *J. Am. Chem. Soc.* **1981**, *103*, 2131.
(14) Wilson, R. M.; Geiser, F. *J. Am. Chem. Soc.* **1978**, *100*, 2225.
(15) Evans, D. F. *J. Chem. Soc.* **1957**, 3151.
(16) Warwick, D. A.; Wells, C. H. *J. Spectrochim. Acta, Part A* **1968**, *24*, 589.
(17) Metcalfe, J.; Rockeley, M. G.; Phillips, D. *J. Chem. Soc., Faraday Trans. 2* **1974**, *70*, 1660.
(18) Brabham, D. E.; Lee, J. *J. Phys. Chem.* **1976**, *80*, 2292.
(19) Morris, D. E.; Tinker, H. B. *Chem. Technol.* **1972**, *2*, 554.
(20) Tinker, H. B.; Morris, D. E. *Rev. Sci. Instrum.* **1972**, *43*, 1024.
(21) Evans, D. F. *J. Chem. Soc.* **1957**, 3885.
(22) Ballintine, T. A.; Schmulbach, C. D. *J. Organometl. Chem.* **1979**, *164*, 381.
(23) Whalley, E. In "High Pressure Chemistry"; Kelm, H., Ed.; D. Reidel: Dordrecht, 1978; pp 127, 131 ff.
(24) Mirbach, M. J. Doctoral Thesis, RWTH Aachen (F.R. Germany), 1976.
(25) Lakowicz, J. R.; Weber, G. *Biochemistry* **1973**, *12*, 4161.
(26) Rotkiewicz, K.; Grabowski, Z. R.; Jasny, J. *Chem. Phys. Lett.* **1975**, *34*, 55.
(27) Jasny, J. *J. Luminescence* **1978**, *17*, 149.
(28) Grabowski, Z. R.; Bylina, A. *Trans. Faraday Soc.* **1964**, 1131.
(29) Latourette, H. K. (FMC Corp.). U. S. Patent 3,663,393, 1972; *Chem. Abstr.* **1972**, *77*, P34120u.
(30) Saus, A. German Offen. 2,2144,855, 1973; *Chem. Abstr.* **1973**, *80*, 9050a.
(31) Saus, A. *CZ-Chem.-Tech.* **1973**, *2*, 19.
(32) Rath, H. P. Doctoral Thesis, RWTH Aachen (F.R. Germany), 1974.
(33) Gascard, T. Doctoral Thesis, RWTH Aachen (F.R. Germany), 1977.
(34) Mirbach, M. J.; Mirbach, M. F.; Saus, A.; Topalsavoglou, N.; Phu, T. N. *J. Am. Chem. Soc.*, in press.
(35) Saus, A.; Gascard, T., to be published.
(36) Mirbach, M. J.; Mirbach, M. F.; Saus, ,A.; Topalsavoglou, N.; Phu, T. N. *J. Am. Chem. Soc.*, in press.
(37) Stephen, H.; Stephen, T. "Solubilities of Inorganic and Organic Compounds"; Pergamon Press: London: (a) Vol. 1, "Binary Systems", Part 1, 1963; (b) Vol. 1, "Binary Systems", Part 2; (c) Vol. 2, "Ternary Systems", Part 1.
(38) Turro, N. J. "Modern Molecular Photochemistry"; The Benjamin/Cummings Publishing Co.: Menlo Park, CA, 1978: (a) p 193; (b) p 591.
(39) Evans, D. J. *Chem. Soc.* **1959**, 2753.
(40) Evans, D. *J. Chem. Soc.* **1960**, 1735.
(41) Evans, D. *J. Chem. Soc.* **1961**, 1987.
(42) Evans, D. F. "Optische Anregung Org. Systeme, 2nd International Farbensymposium, Schloss Elmau, Germany"; Jung, W., Ed.; Verlag Chemie: Weinheim, 1964; p 586.
(43) Lamola, A. A.; Hammond, G. S. *J. Chem. Phys.* **1965**, *43*, 2129.
(44) Kellogg, R. E.; Simpson, W. T. *J. Am. Chem. Soc.* **1965**, *87*, 4230.
(45) Grabowska, A. *Chem. Phys. Lett.* **1967**, *1*, 113.
(46) Bylina, A. *Chem. Phys. Lett.* **1968**, *1*, 509.
(47) Metcalfe, J.; Chervinsky, S.; Oref, I. *Chem. Phys. Lett.* **1976**, *42*, 190.
(48) Mirbach, M. F. Doctoral Thesis, RWTH Aachen (F.R. Germany), 1976.
(49) Crosby, P. M.; Dyke, J. M.; Metcalfe, J.; Rest, A. J.; Salisbury, K.; Sodeau, J. R. *J. Chem. Soc., Perkin Trans. 2*, **1977**, 182.
(50) Alder, L.; Gloyna, D.; Wegener, W.; Pragst, F.; Henning, H.-G. *Chem. Phys. Lett.* **1979**, *64*, 503.
(51) Turro, N. J.; Cherry, W. R.; Mirbach, M. J.; Mirbach, M. F.; Ramamurthy, V. *Mol. Photochem.* **1978/1979**, *9*, 111.
(52) Grabowska, A.; Pakula, B. *Proc. Int. Conf. Lumin.* **1966**, 368.
(53) Dijkgraaf, C.; Sitters, R.; Hoytink, G. J. *Mol. Phys.* **1962**, *5*, 643.
(54) Evans, D. F.; Tucker, J. N. *J. Chem. Soc., Faraday Trans. 2* **1972**, *68*, 174.
(55) Kasha, M. "Singlet Molecular Oxygen"; Tokyo Science University Lectures, 1979.
(56) Evans, D. F. *J. Chem. Soc. D* **1969**, 367.

(57) Evans, D. F.; Tucker, J. N. *J. Chem. Soc., Faraday Trans. 2* **1976**, *72*, 1661.
(58) Matheson, I. B. C.; Massoudi, R. *J. Am. Chem. Soc.* **1980**, *102*, 1942.
(59) Bylina, A.; Grabowski, Z. R. *Trans. Faraday Soc.* **1969**, *65*, 458.
(60) Lakowicz, J. R.; Weber, G. *Biochemistry* **1973**, *12*, 4171.
(61) Weber, G.; Lakowicz, J. R. *Chem. Phys. Lett.* **1973**, *22*, 419.
(62) Kirkor-Kaminska, E.; Rotkiewicz, K.; Grabowska, A. *Chem. Phys. Lett.* **1978**, *58*, 379.
(63) Clark, W. D. K.; Steel, C. *J. Am. Chem. Soc.* **1971**, *93*, 6347.
(64) (a) Wilson, R. M.; Moats, D.; Rekers, J. W. VIIIth IUPAC Symposium on Photochemistry, Seefeld, Austria, 1980, Contributed Paper No. 174. (b) Wilson, R. M., private communication.
(65) Kemula, W.; Grabowska, A. *Bull. Acad. Polon. Sci., Ser. Sci. Chim.* **1960**, *8*, 525.
(66) Kemula, W.; Grabowska, A. *Nature (London)* **1960**, *188*, 224.
(67) Nasielski, J.; Kirsch, P.; Wilputte-Steinert, L. *J. Organomet. Chem.* **1971**, *27*, C13.
(68) Wrighton, M.; Schroeder, M. A. *J. Am. Chem. Soc.* **1973**, *95*, 5764.
(69) (a) Mirbach, M. J.; van de Berg, A.; Saus, A., Unpublished results. (b) Mirbach, M. J. Habilitation-Thesis, University of Duisburg (F.R. Germany), 1982.
(70) (a) Platbrood, G.; Wilputte-Steinert, L. *J. Organomet. Chem.* **1974**, *70*, 393. (b) Platbrood, G.; Wilputte-Steinert, L. *Bull. Soc. Chim. Belg.* **1973**, *82*, 733.
(71) Mirbach, M. J.; Steinmetz, D.; Saus, A. *J. Organomet. Chem.* **1979**, *168*, C13.
(72) (a) Mirbach, M. J.; Phu, T. N.; Saus, A., unpublished results. (b) Mirbach, M. J.; Phu, T. N.; Saus, A. GDCh Conference on Photochemistry, Göttingen (F.R. Germany), 1979.
(73) Phu, T. N. Doctoral Thesis, University of Duisburg (F. R. Germany), 1982.
(74) Mirbach, M. F.; Turro, N. J., unpublished results.
(75) For a survey on the hydroformylation reaction, see: Pruett, R. L. *Adv. Organomet. Chem.* **1979**, *17*, 1.
(76) Mirbach, M. J.; Topalsavoglu, N.; Phu, T. N.; Mirbach, M. F.; Saus, A. *Angew. Chem., Int. Ed. Engl.* **1981**, *20*, 381.
(77) Mirbach, M. J.; Phu, T. N.; Topalsavoglou, N.; Mirbach, M. F.; Saus, A. VIIIth IUPAC Symposium on Photochemistry, Seefeld, Austria, 1980, Contributed Paper No. 116.
(78) Mirbach, M. J.; Phu, T. N.; Topalsavoglou, N.; Saus, A. 2nd International Symposium on Homogeneous Catalysis, Düsseldorf (F.R. Germany), 1980, Abstracts of Papers, p 70.
(79) Mirbach, M. J.; Mirbach, M. F.; Saus, A.; Topalsavoglou, N.; Phu, T. N. Xth International Conference on Organometallic Chemistry, Toronto, 1981, Book of Abstracts 1C10, p 49.
(80) Mirbach, M. J.; Mirbach, M. F.; Phu, T. N.; Saus, A., to be published.
(81) Cote, W. J.; Krusic, P. J. Xth International Conference on Organometallic Chemistry, Toronto, Canada, 1981, Book of Abstracts 1C09, p 48.
(82) Miller, S. A. "Ethylene"; E. Benn, Ltd.: London, 1969.
(83) Mirbach, M. F.; Mirbach, M. J.; Saus, A. *Z. Naturforsch. B: Anorg. Chem., Org. Chem.* **1977**, 32B, 47.
(84) Bryce-Smith, D.; Gilbert, A.; Orger, B.; Tyrell, H. *J. Chem. Soc., Chem. Commun.* **1974**, 334.
(85) Mirbach, M. F.; Mirbach, M. J.; Saus, A. *Tetrahedron Lett.* **1977**, 959.
(86) Mirbach, M. J.; Mirbach, M. F.; Saus, A. EUCHEM Conference on Useful Aspects of Photochemistry, Ghent, Belgium, 1975.
(87) Rath, H. P.; Saus, A.; Dederichs, B. *Z. Naturforsch. B: Anorg. Chem., Org. Chem.* **1975**, 30B, 740.
(88) Gascard, T.; Dederichs, B.; Saus, A. *Tenside Deterg.* **1981**, 18, 17.
(89) Kaefer, P.; Saus, A.; Dederichs, B. *Z. Naturforsch. B: Anorg. Chem., Org. Chem.* **1977**, 32B, 58.
(90) Gascard, T.; Saus, A. *Erdöl Kohle, Erdgas, Petrochem.* **1979**, *32*, 178.
(91) Grabowska, A. *Spectrochim. Acta* **1963**, *19*, 307.
(92) Calcaterra, L. T.; Schuster, D. I. *J. Am. Chem. Soc.* **1981**, *103*, 2460.
(93) Dalton, J. C.; Shen, M.; Snyder, J. J. *J. Am. Chem. Soc.* **1976**, *98*, 5023.
(94) Schuster, D. I.; Eriksen, J.; Engel, P. S.; Schexnayder, M. S. *J. Am. Chem. Soc.* **1976**, *98*, 5025.
(95) Mirbach, M. J.; Henne, A.; Schaffner, K. *J. Am. Chem. Soc.* **1978**, *100*, 7127.
(96) Koltzenburg, G.; Fuss, P. G.; Leitich, J. *Tetrahedron Lett.* **1966**, 3409.
(97) Grabowska, A. *J. Mol. Spectrosc.* **1966**, *20*, 96.